J|A|C|S ARTICLES

Published on Web 02/18/2010

Combining Very Large Quadratic and Cubic Nonlinear Optical Responses in Extended, Tris-Chelate Metallochromophores with Six π-Conjugated Pyridinium Substituents

Benjamin J. Coe,*[,†] John Fielden,[†] Simon P. Foxon,[†] Bruce S. Brunschwig,[‡] Inge Asselberghs,[§] Koen Clays,[§] Anna Samoc,[||] and Marek Samoc[||,⊥]

School of Chemistry, University of Manchester, Oxford Road, Manchester M13 9PL, U.K., Molecular Materials Research Center, Beckman Institute, MC 139-74, California Institute of Technology, 1200 East California Boulevard, Pasadena, California 91125, Department of Chemistry, University of Leuven, Celestijnenlaan 200D, B-3001 Leuven, Belgium, Laser Physics Centre, Research School of Physics and Engineering, Australian National University, Canberra, Australian Capital Territory 0200, Australia, and Institute of Physical and Theoretical Chemistry, Wrocław University of Technology, Wybrzeże Wyspiańskiego 27, 50-370 Wrocław, Poland

Received December 14, 2009; E-mail: b.coe@manchester.ac.uk

Abstract: We describe a series of nine new complex salts in which electron-rich Ru^{II} or Fe^{II} centers are connected via π-conjugated bridges to six electron-accepting *N*-methyl-/*N*-arylpyridinium groups. This work builds upon our previous preliminary studies (Coe, B. J. *J. Am. Chem. Soc.* **2005**, *127*, 13399−13410; *J. Phys. Chem. A* **2007**, *111*, 472−478), with the aims of achieving greatly enhanced NLO properties and also combining large quadratic and cubic effects in potentially redox-switchable molecules. Characterization has involved various techniques, including electronic absorption spectroscopy and cyclic voltammetry. The complexes display intense, visible d $\rightarrow \pi^*$ metal-to-ligand charge-transfer (MLCT) bands, and their $\pi \rightarrow \pi^*$ intraligand charge-transfer (ILCT) absorptions in the near-UV region show molar extinction coefficients as high as ca. 3.5×10^5 M^{-1} cm^{-1}. Molecular quadratic nonlinear optical (NLO) responses β have been determined by using hyper-Rayleigh scattering at 800 and 1064 nm and also via Stark (electroabsorption) spectroscopic studies. The directly and indirectly derived β values are very large, with the Stark-based static first hyperpolarizabilities β_0 reaching as high as ca. 10^{-27} esu, and generally increase on extending the π-conjugation and enhancing the electron-accepting strength of the ligands. Cubic NLO properties have also been measured by using the Z-scan technique, revealing relatively high two-photon absorption cross sections of up to 2500 GM at 750 nm.

Introduction

The promise of diverse applications, including optical data processing and biological imaging, has stimulated many studies with organic nonlinear optical (NLO) materials over recent years.[1] For example, NLO effects allow the manipulation of laser light beams and may thus form the basis of all-optical computing devices. Although purely organic compounds have received most attention, transition metal coordination and organometallic complexes are especially interesting in this context. Such compounds offer unparalleled structural diversity and scope for the creation of multifunctional optical materials,[2] featuring for example redox-switchable NLO responses.[3]

Most NLO chromophores comprise relatively simple dipolar electronic structures, but octupolar compounds have also attracted considerable interest, especially for potential quadratic (second-order) applications.[4] Octupolar molecules have zero net ground-state dipole moments, but large dipole moment changes accompanying intramolecular charge-transfer (ICT) excitations can lead to substantial values of the first hyperpolarizability β, which governs quadratic NLO effects at the molecular level. Molecules with large two-photon absorption (2PA) cross sections σ_2 are of major interest for a wide range of potential applications, including optical power limiting, two-photon upconversion lasing, 3D optical data storage, and photodynamic cancer therapy.[5] The quantity σ_2 is related to the imaginary part of the second hyperpolarizability γ, and the latter is the origin of cubic NLO responses. It is established that large γ and σ_2 values require extended conjugated π-systems, and recent studies

† University of Manchester.
‡ California Institute of Technology.
§ University of Leuven.
|| Australian National University.
⊥ Wrocław University of Technology.

(1) (a) Zyss, J. *Molecular Nonlinear Optics: Materials, Physics and Devices*; Academic Press: Boston, 1994. (b) Bosshard, Ch.; Sutter, K.; Prêtre, Ph.; Hulliger, J.; Flörsheimer, M.; Kaatz, P.; Günter, P. *Organic Nonlinear Optical Materials*; Gordon & Breach: Amsterdam, The Netherlands, 1995; Advances in Nonlinear Optics Vol. 1. (c) *Nonlinear Optics of Organic Molecules and Polymers*; Nalwa, H. S., Miyata, S., Eds.; CRC Press: Boca Raton, FL, 1997. (d) Marder, S. R. *Chem. Commun.* **2006**, 131–134. (e) *Nonlinear Optical Properties of Matter: From Molecules to Condensed Phases*; Papadopoulos, M. G., Leszczynski, J., Sadlej, A. J., Eds.; Springer: Dordrecht, The Netherlands, 2006.

 10.1021/ja910538s

have featured various branched structures, including octupolar chromophores.[6]

Zyss et al. first highlighted the octupolar nature of D_3 tris-chelate transition metal complexes, using hyper-Rayleigh scattering (HRS) measurements and a three-state theoretical model to derive reasonably large static first hyperpolarizabilities β_0 of ca. 50×10^{-30} esu for the salts $[Ru^{II}(bpy)_3]Br_2$ (bpy = 2,2′-bipyridyl) and $[Ru^{II}(phen)_3]Cl_2$ (phen = 1,10-phenanthroline).[7] An off-resonance β_0 response is the quantity that is of most relevance to quadratic NLO applications, because these normally require the avoidance of any actual light absorption. Later HRS studies on a $[Ru^{II}(bpy)_3]^{2+}$ derivative with six electron-donating styryl substituents revealed a huge β_0 value of 2200×10^{-30} esu.[8] However, other workers found that this β_0 value is overestimated due to contributions from 2PA-induced luminescence,[9] and subsequent investigations have thus given a smaller (albeit still large) β_0 value of 380×10^{-30} esu for this complex.[10] A number of other quadratic NLO studies have been carried out with derivatives of $[Ru^{II}(bpy)_3]^{2+}$ and related complexes of other metals.[2n,10,11] Very recent reports concerning such chromophores have also focused on their 2PA properties, from both a largely experimental perspective[12] and purely theoretical analyses.[13]

(2) (a) Kanis, D. R.; Ratner, M. A.; Marks, T. J. *Chem. Rev.* **1994**, *94*, 195–242. (b) Long, N. J. *Angew. Chem., Int. Ed. Engl.* **1995**, *34*, 21–38. (c) Whittall, I. R.; McDonagh, A. M.; Humphrey, M. G.; Samoc, M. *Adv. Organomet. Chem.* **1998**, *42*, 291–362. (d) Whittall, I. R.; McDonagh, A. M.; Humphrey, M. G.; Samoc, M. *Adv. Organomet. Chem.* **1998**, *43*, 349–405. (e) Heck, J.; Dabek, S.; Meyer-Friedrichsen, T.; Wong, H. *Coord. Chem. Rev.* **1999**, *190*−*192*, 1217–1254. (f) Gray, G. M.; Lawson, C. M. In *Optoelectronic Properties of Inorganic Compounds*; Roundhill, D. M., Fackler, J. P., Jr., Eds.; Plenum: New York, 1999; pp 1−27. (g) Shi, S. In *Optoelectronic Properties of Inorganic Compounds*; Roundhill, D. M., Fackler, J. P., Jr., Eds.; Plenum: New York, 1999; pp 55−105. (h) Le Bozec, H.; Renouard, T. *Eur. J. Inorg. Chem.* **2000**, 229–239. (i) Barlow, S.; Marder, S. R. *Chem. Commun.* **2000**, 1555–1562. (j) Lacroix, P. G. *Eur. J. Inorg. Chem.* **2001**, 339–348. (k) Di Bella, S. *Chem. Soc. Rev.* **2001**, *30*, 355–366. (l) Goovaerts, E.; Wenseleers, W. E.; Garcia, M. H.; Cross, G. H. In *Handbook of Advanced Electronic and Photonic Materials and Devices*; Nalwa, H. S., Ed.; Academic Press: San Diego, CA, 2001; Vol. 9, pp 127−191. (m) Coe, B. J. In *Comprehensive Coordination Chemistry II*; McCleverty, J. A., Meyer, T. J., Eds.; Elsevier Pergamon: Oxford, U.K., 2004; Vol. 9, pp 621−687. (n) Maury, O.; Le Bozec, H. *Acc. Chem. Res.* **2005**, *38*, 691–704. (o) Cariati, E.; Pizzotti, M.; Roberto, D.; Tessore, F.; Ugo, R. *Coord. Chem. Rev.* **2006**, *250*, 1210–1233. (p) Coe, B. J. *Acc. Chem. Res.* **2006**, *39*, 383–393. (q) Thompson, M. E.; Djurovich, P. E.; Barlow, S.; Marder, S. In *Comprehensive Organometallic Chemistry III*; Crabtree, R. H., Mingos, D. M. P., Eds.; Elsevier: Oxford, U.K., 2006; Vol. 12, pp. 101−194. (r) Zhang, C.; Song, Y.-L.; Wang, X. *Coord. Chem. Rev.* **2007**, *251*, 111–141. (s) Andraud, C.; Maury, O. *Eur. J. Inorg. Chem.* **2009**, 4357–4371.

(3) (a) Coe, B. J.; Houbrechts, S.; Asselberghs, I.; Persoons, A. *Angew. Chem., Int. Ed.* **1999**, *38*, 366–369. (b) Weyland, T.; Ledoux, I.; Brasselet, S.; Zyss, J.; Lapinte, C. *Organometallics* **2000**, *19*, 5235–5237. (c) Malaun, M.; Reeves, Z. R.; Paul, R. L.; Jeffery, J. C.; McCleverty, J. A.; Ward, M. D.; Asselberghs, I.; Clays, K.; Persoons, A. *Chem. Commun.* **2001**, 49–50. (d) Malaun, M.; Kowallick, R.; McDonagh, A. M.; Marcaccio, M.; Paul, R. L.; Asselberghs, I.; Clays, K.; Persoons, A.; Bildstein, B.; Fiorini, C.; Nunzi, J.-M.; Ward, M. D.; McCleverty, J. A. *Dalton Trans.* **2001**, 3025–3038. (e) Cifuentes, M. P.; Powell, C. E.; Humphrey, M. G.; Heath, G. A.; Samoc, M.; Luther-Davies, B. *J. Phys. Chem. A* **2001**, *105*, 9625–9627. (f) Paul, F.; Costuas, K.; Ledoux, I.; Deveau, S.; Zyss, J.; Halet, J.-F.; Lapinte, C. *Organometallics* **2002**, *21*, 5229–5235. (g) Powell, C. E.; Cifuentes, M. P.; Morrall, J. P.; Stranger, R.; Humphrey, M. G.; Samoc, M.; Luther-Davies, B.; Heath, G. A. *J. Am. Chem. Soc.* **2003**, *125*, 602–610. (h) Asselberghs, I.; Clays, K.; Persoons, A.; McDonagh, A. M.; Ward, M. D.; McCleverty, J. A. *Chem. Phys. Lett.* **2003**, *368*, 408–411. (i) Powell, C. E.; Humphrey, M. G.; Cifuentes, M. P.; Morrall, J. P.; Samoc, M.; Luther-Davies, B. *J. Phys. Chem. A* **2003**, *107*, 11264–11266. (j) Sporer, C.; Ratera, I.; Ruiz-Molina, D.; Zhao, Y.-X.; Vidal-Gancedo, J.; Wurst, K.; Jaitner, P.; Clays, K.; Persoons, A.; Rovira, C.; Veciana, J. *Angew. Chem., Int. Ed.* **2004**, *43*, 5266–5268. (k) Cifuentes, M. P.; Powell, C. E.; Morrall, J. P.; McDonagh, A. M.; Lucas, N. T.; Humphrey, M. G.; Samoc, M.; Houbrechts, S.; Asselberghs, I.; Clays, K.; Persoons, A.; Isoshima, T. *J. Am. Chem. Soc.* **2006**, *128*, 10819–10832. (l) Samoc, M.; Gauthier, N.; Cifuentes, M. P.; Paul, F.; Lapinte, C.; Humphrey, M. G. *Angew. Chem., Int. Ed.* **2006**, *45*, 7376–7379. (m) Dalton, G. T.; Cifuentes, M. P.; Petrie, S.; Stranger, R.; Humphrey, M. G.; Samoc, M. *J. Am. Chem. Soc.* **2007**, *129*, 11882–11883. (n) Boubekeur-Lecaque, L.; Coe, B. J.; Clays, K.; Foerier, S.; Verbiest, T.; Asselberghs, I. *J. Am. Chem. Soc.* **2008**, *130*, 3286–3287. (o) Wahab, A.; Bhattacharya, M.; Ghosh, S.; Samuelson, A. G.; Das, P. K. *J. Phys. Chem. B* **2008**, *112*, 2842–2847.

(4) Selected examples: (a) Ledoux, I.; Zyss, J.; Siegel, J. S.; Brienne, J.; Lehn, J.-M. *Chem. Phys. Lett.* **1990**, *172*, 440–444. (b) Joffre, M.; Yaron, D.; Silbey, R. J.; Zyss, J. *J. Chem. Phys.* **1992**, *97*, 5607–5615. (c) Verbiest, T.; Clays, K.; Persoons, A.; Meyers, F.; Brédas, J. L. *Opt. Lett.* **1993**, *18*, 525–527. (d) Zyss, J. *J. Chem. Phys.* **1993**, *98*, 6583–6599. (e) Verbiest, T.; Clays, K.; Samyn, C.; Wolff, J.; Reinhoudt, D.; Persoons, A. *J. Am. Chem. Soc.* **1994**, *116*, 9320–9323. (f) Zyss, J.; Ledoux, I. *Chem. Rev.* **1994**, *94*, 77–105. (g) Wolff, J. J.; Wortmann, R. *Adv. Phys. Org. Chem.* **1999**, *32*, 121–217. (h) Wolff, J. J.; Siegler, F.; Matschiner, R.; Wortmann, R. *Angew. Chem., Int. Ed.* **2000**, *39*, 1436–1439. (i) Cho, B. R.; Piao, M. J.; Son, K. H.; Lee, S. H.; Yoon, S. J.; Jeon, S.-J.; Cho, M.-H. *Chem. Eur. J.* **2002**, *8*, 3907–3916. (j) Brunel, J.; Mongin, O.; Jutand, A.; Ledoux, I.; Zyss, J.; Blanchard-Desce, M. *Chem. Mater.* **2003**, *15*, 4139–4148. (k) Cui, Y. Z.; Fang, Q.; Lei, H.; Xue, G.; Yu, W. T. *Chem. Phys. Lett.* **2003**, *377*, 507–511. (l) Ray, P. C.; Leszczynski, J. *Chem. Phys. Lett.* **2004**, *399*, 162–166. (m) Claessens, C. G.; González-Rodríguez, D.; Torres, T.; Martín, G.; Agulló-Lopez, F.; Ledoux, I.; Zyss, J.; Ferro, V. R.; García de la Vega, J. M. *J. Phys. Chem. B* **2005**, *109*, 3800–3806. (n) Le Floch, V.; Brasselet, S.; Zyss, J.; Cho, B. R.; Lee, S. H.; Jeon, S.-J.; Cho, M.-H.; Min, K. S.; Suh, M. P. *Adv. Mater.* **2005**, *17*, 196–200. (o) Jeong, M.-Y.; Kim, H. M.; Jeon, S.-J.; Brasselet, S.; Cho, B. R. *Adv. Mater.* **2007**, *19*, 2107–2111. (p) Liu, Y.; Xu, X.; Zheng, F.; Cui, Y. *Angew. Chem., Int. Ed.* **2008**, *47*, 4538–4541. (q) Kim, H. M.; Cho, B. R. *J. Mater. Chem.* **2009**, *19*, 7402–7409.

(5) Selected examples: (a) Wang, C.; Wang, X.-M.; Shao, Z.-S.; Zhao, X.; Zhou, G.-Y.; Wang, D.; Fang, Q.; Jiang, M.-H. *Appl. Opt.* **2001**, *40*, 2475–2478. (b) Zheng, Q.-D.; He, G. S.; Lin, T.-C.; Prasad, P. N. *J. Mater. Chem.* **2003**, *13*, 2499–2504. (c) He, G. S.; Lin, T.-C.; Prasad, P. N.; Cho, C.-C.; Yu, L.-J. *Appl. Phys. Lett.* **2003**, *82*, 4717–4719. (d) Yang, Z.; Wu, Z.-K.; Ma, J.-S.; Xia, A.-D.; Li, Q.-S.; Liu, C.-L.; Gong, Q.-H. *Appl. Phys. Lett.* **2005**, *86*, 061903. (e) Samoc, M.; Morrall, J. P.; Dalton, G. T.; Cifuentes, M. P.; Humphrey, M. G. *Angew. Chem., Int. Ed.* **2007**, *46*, 731–733. (f) Terenziani, F.; Katan, C.; Badaeva, E.; Tretiak, S.; Blanchard-Desce, M. *Adv. Mater.* **2008**, *20*, 4641–4678. (g) Jana, A.; Jang, S. Y.; Shin, J.-Y.; De, A. K.; Goswami, D.; Kim, D.; Bharadwaj, P. J. *Chem. Eur. J.* **2008**, *14*, 10628–10638. (h) D'Aléo, A.; Picot, A.; Baldeck, P. L.; Andraud, C.; Maury, O. *Inorg. Chem.* **2008**, *47*, 10269–10279. (i) He, G. S.; Tan, L.-S.; Zheng, Q.-D.; Prasad, P. N. *Chem. Rev.* **2008**, *108*, 1245–1330. (j) Collings, J. C.; Poon, S.-Y.; Le Droumaguet, C.; Charlot, M.; Katan, C.; Pålsson, L.-O.; Beeby, A.; Mosely, J. A.; Kaiser, H. M.; Kaufmann, D.; Wong, W.-Y.; Blanchard-Desce, M.; Marder, T. B. *Chem. Eur. J.* **2009**, *15*, 198–208. (k) Pawlicki, M.; Collins, H. A.; Denning, R. G.; Anderson, H. L. *Angew. Chem., Int. Ed.* **2009**, *48*, 3244–3266. (l) Dvornikov, A. S.; Walker, E. P.; Rentzepis, P. M. *J. Phys. Chem. A* **2009**, *113*, 13633–13644.

(6) Selected examples: (a) Lee, W.-H.; Lee, H.-C.; Kim, J.-A.; Choi, J.-H.; Cho, M.-H.; Jeon, S.-J.; Cho, B. R. *J. Am. Chem. Soc.* **2001**, *123*, 10658–10667. (b) Beljonne, D.; Wenseleers, W.; Zojer, E.; Shuai, Z.-G.; Vogel, H.; Pond, S. J. K.; Perry, J. W.; Marder, S. R.; Bredas, J.-L. *Adv. Funct. Mater.* **2002**, *12*, 631–641. (c) Kannan, R.; He, G. S.; Lin, T.-C.; Prasad, P. N.; Vaia, R. A.; Tan, L.-S. *Chem. Mater.* **2004**, *16*, 185–194. (d) Ray, P. C.; Leszczynski, J. *J. Phys. Chem. A* **2005**, *109*, 6689–6696. (e) Zhou, X.; Feng, J.-K.; Ren, A.-M. *Chem. Phys. Lett.* **2005**, *403*, 7–15. (f) Easwaramoorthi, S.; Shin, J.-Y.; Cho, S.; Kim, P.-S.; Inokuma, Y.; Tsurumaki, E.; Osuka, A.; Kim, D.-H. *Chem. Eur. J.* **2009**, *15*, 12005–12017. (g) Kim, H. M.; Seo, M. S.; Jeon, S.-J.; Cho, B. R. *Chem. Commun.* **2009**, 7422–7424.

(7) Zyss, J.; Dhenaut, C.; Chauvan, T.; Ledoux, I. *Chem. Phys. Lett.* **1993**, *206*, 409–414.

(8) Dhenaut, C.; Ledoux, I.; Samuel, I. D. W.; Zyss, J.; Bourgault, M.; Le Bozec, H. *Nature* **1995**, *374*, 339–342.

(9) Morrison, I. D.; Denning, R. G.; Laidlaw, W. M.; Stammers, M. A. *Rev. Sci. Instrum.* **1996**, *67*, 1445–1453.

(10) Le Bozec, H.; Renouard, T.; Bourgault, M.; Dhenaut, C.; Brasselet, S.; Ledoux, I.; Zyss, J. *Synth. Met.* **2001**, *124*, 185–189.

While $[M^{II}(bpy)_3]^{2+}$ (M = Fe, Ru, Zn, etc.) complex units themselves have octupolar ground states, they form dipolar ICT excited states. Polarized HRS and Stark spectroscopic measurements have shown that the β responses of $[Ru^{II}(bpy)_3]^{2+}$ derivatives hexasubstituted with electron-donating styryl groups are dominated by multiple degenerate dipolar intraligand charge-transfer (ILCT) excitations, rather than an octupolar transition.[14] These ILCT transitions are red-shifted by metal coordination and are directionally opposed to the metal-to-ligand charge-transfer (MLCT) excitations.[10,14] Since all previous NLO studies with this class of tris-chelate complexes have involved electron-donor-substituted species,[2n,10–14] we recently prepared a series of $[M^{II}(bpy)_3]^{2+}$ (M = Fe, Ru) derivatives bearing electron-withdrawing pyridinium groups and carried out quadratic[15] and cubic[16] NLO investigations. In these complexes, the MLCT transitions are expected to dominate the NLO responses because the ILCT processes, despite also being directed toward the pyridinium units, occur at very short wavelengths (below about 330 nm). The present report concerns extended relatives of our previously reported chromophores, with the aim being to achieve greatly enhanced quadratic and cubic NLO properties. The contributions of the ILCT transitions to the β responses become more significant in these new complexes and are even amenable to assessment by Stark spectroscopy in two cases.

Experimental Section

Materials and Procedures. The compounds *cis*-$Ru^{II}Cl_2(DMSO)_4$,[17] 4,4′-bis[(diethoxyphosphinyl)methyl]-2,2′-bipyridyl,[18] 2,2′-bipyridyl-4,4′-dicarboxaldehyde,[19] *N*-phenyl-4-picolinium chloride hydrate ([Phpic$^+$]Cl·1.25H_2O),[20] (*E*)-3-(4-pyridyl)-2-propenal,[21] and 4-[(*E*)-2-(4-pyridyl)vinyl]benzaldehyde[22] were prepared according to published procedures. All other reagents were obtained commercially and used as supplied. Products were dried overnight in a vacuum desiccator ($CaSO_4$) prior to characterization.

General Physical Measurements. ^{1}H NMR spectra were recorded on a Bruker 400 MHz spectrometer, and all shifts are quoted with respect to TMS. The fine splitting of pyridyl or phenyl ring AA′BB′ patterns is ignored, and the signals are reported as simple doublets, with *J* values referring to the two most intense peaks. Elemental analyses were performed by the Microanalytical Laboratory, University of Manchester, using a Carlo Erba EA1108 instrument. UV−vis spectra were obtained by using a Shimadzu UV-2401 PC spectrophotometer, and mass spectra were recorded by using electron impact on a Micromass Trio 2000 or positive electrospray on a Micromass Platform II spectrometer. Luminescence spectra were recorded on a Gilden photonics fluoroSENS fluorimeter. Cyclic voltammetric measurements were performed by using an EG&G PAR Model 283 potentiostat/galvanostat. A single-compartment cell was used with a silver/silver chloride reference electrode (3 M NaCl, saturated AgCl) separated by a salt bridge from a 2 mm glassy-carbon-disk working electrode and Pt-wire auxiliary electrode. Acetonitrile was freshly distilled (from CaH_2), and $[N(C_4H_9\text{-}n)_4]PF_6$, as supplied from Fluka, was used as the supporting electrolyte. Solutions containing ca. 10^{-3} M analyte (0.1 M electrolyte) were deaerated by purging with N_2. All $E_{1/2}$ values were calculated from $(E_{pa} + E_{pc})/2$ at a scan rate of 200 mV s^{-1}.

Synthesis of 4,4′-Bis[(*E*)-2-(4-pyridyl)vinyl]-2,2′-bipyridyl, bbpe. Potassium *tert*-butoxide (624 mg, 5.56 mmol) was added to a stirred solution of 4,4′-bis-[(diethoxyphosphinyl)methyl]-2,2′-bipyridyl (1.00 g, 2.19 mmol) and 4-pyridinecarboxaldehyde (528 mg, 4.93 mmol) in tetrahydrofuran (40 mL). The reaction vessel was sealed and protected from the light, and the contents were stirred at room temperature for 2 h. Distilled water (60 mL) was added, and the reaction mixture was stirred for a further 2 min. The cream-colored solid was filtered off, washed with copious amounts of water followed by diethyl ether, and dried: yield 681 mg, 84%. ^{1}H NMR δ_H ($CDCl_3$): 8.72 (2 H, d, J = 5.1 Hz, C_5H_3N), 8.64 (4 H, d, J = 6.1 Hz, C_5H_4N), 8.60 (2 H, s, C_5H_3N), 7.45−7.41 (6 H, C_5H_3N + C_5H_4N), 7.39 (2 H, d, J = 16.5 Hz, CH), 7.32 (2 H, d, J = 16.4 Hz, CH). Anal. Calcd for $C_{24}H_{18}N_4$·0.5H_2O: C, 77.61; H, 5.16; N, 15.08. Found: C, 77.80; H, 4.89; N, 15.05. EI-MS: *m*/*z* 363 ([MH]$^+$).

Synthesis of 4,4′-Bis[(*E*)-2-(*N*-methyl-4-pyridyl)vinyl]-2,2′-bipyridyl Iodide, [Me_2bbpe^{2+}]I_2. A mixture of bbpe·0.5H_2O (303 mg, 0.816 mmol) and iodomethane (10 mL) in acetone (40 mL) was heated at reflux in the dark for 4 h. The orange precipitate was filtered off, washed with a small amount of acetone followed by copious amounts of CH_2Cl_2 and then diethyl ether, and dried: yield 454 mg, 84%. ^{1}H NMR δ_H (CD_3SOCD_3): 8.98 (4 H, d, J = 6.8 Hz, C_5H_4N), 8.86 (2 H, d, J = 5.2 Hz, C_5H_3N), 8.74 (2 H, s, C_5H_3N), 8.37 (4 H, d, J = 6.8 Hz, C_5H_4N), 8.16 (2 H, d, J = 16.4 Hz, CH), 7.91 (2 H, d, J = 16.4 Hz, CH), 7.81 (2 H, dd, J = 5.0, 1.4 Hz, C_5H_3N), 4.30 (6 H, s, Me). Anal. Calcd for $C_{26}H_{24}I_2N_4$·0.7H_2O: C, 47.39; H, 3.89; N, 8.50. Found: C, 47.44; H, 3.61; N, 8.45. ES-MS: *m*/*z* 519 ([M − I]$^+$).

Synthesis of 4,4′-Bis[(*E*)-2-(*N*-methyl-4-pyridyl)vinyl]-2,2′-bipyridyl Hexafluorophosphate, [Me_2bbpe^{2+}][PF_6]$_2$. [Me_2bbpe^{2+}]I_2·0.7H_2O (446 mg, 0.677 mmol) was dissolved in 2/1 methanol/water. Slow addition of aqueous NH_4PF_6 (0.6 M) followed by water (50 mL) gave a white precipitate, which was filtered off, washed with copious amounts of water and then diethyl ether, and dried: yield 433 mg, 92%. ^{1}H NMR δ_H (CD_3SOCD_3): 8.97 (4 H, d, J = 6.6 Hz, C_5H_4N), 8.86 (2 H, d, J = 5.0 Hz, C_5H_3N), 8.75 (2 H, s,

(11) Selected examples: (a) Le Bouder, T.; Maury, O.; Le Bozec, H.; Ledoux, I.; Zyss, J. *Chem. Commun.* **2001**, 2430–2431. (b) Le Bozec, H.; Le Bouder, T.; Maury, O.; Bondon, A.; Ledoux, I.; Deveau, S.; Zyss, J. *Adv. Mater.* **2001**, *13*, 1677–1681. (c) Sénéchal, K.; Maury, O.; Le Bozec, H.; Ledoux, I.; Zyss, J. *J. Am. Chem. Soc.* **2002**, *124*, 4560–4561. (d) Le Bouder, T.; Maury, O.; Bondon, O.; Costuas, K.; Amouyal, E.; Ledoux, I.; Zyss, J.; Le Bozec, H. *J. Am. Chem. Soc.* **2003**, *125*, 12284–12299. (e) Viau, L.; Bidault, S.; Maury, O.; Brasselet, S.; Ledoux, I.; Zyss, J.; Ishow, E.; Nakatani, K.; Le Bozec, H. *J. Am. Chem. Soc.* **2004**, *126*, 8386–8387. (f) Maury, O.; Viau, L.; Sénéchal, K.; Corre, B.; Guégan, J.-P.; Renouard, T.; Ledoux, I.; Zyss, J.; Le Bozec, H. *Chem. Eur. J.* **2004**, *10*, 4454–4466. (g) Bidault, S.; Brasselet, S.; Zyss, J.; Maury, O.; Le Bozec, H. *J. Chem. Phys.* **2007**, *126*, 034312-1–034312-13.

(12) (a) Girardot, C.; Lemercier, G.; Mulatier, J.-C.; Chauvin, J.; Baldeck, P. L.; Andraud, C. *Dalton Trans.* **2007**, 3421–3426. (b) Feuvrie, C.; Maury, O.; Le Bozec, H.; Ledoux, I.; Morrall, J. P.; Dalton, G. T.; Samoc, M.; Humphrey, M. G. *J. Phys. Chem. A* **2007**, *111*, 8980–8985. (c) Boca, S. C.; Four, M.; Bonne, A.; van der Sanden, B.; Astilean, S.; Baldeck, P. L.; Lemercier, G. *Chem. Commun.* **2009**, 4590–4592.

(13) (a) Liu, X.-J.; Feng, J.-K.; Ren, A.-M.; Cheng, H.; Zhou, X. *J. Chem. Phys.* **2004**, *120*, 11493–11499. (b) Zhang, X.-B.; Feng, J.-K.; Ren, A.-M. *J. Phys. Chem. A* **2007**, *111*, 1328–1338.

(14) Vance, F. W.; Hupp, J. T. *J. Am. Chem. Soc.* **1999**, *121*, 4047–4053.

(15) Coe, B. J.; Harris, J. A.; Brunschwig, B. S.; Asselberghs, I.; Clays, K.; Garín, J.; Orduna, J. *J. Am. Chem. Soc.* **2005**, *127*, 13399–13410.

(16) Coe, B. J.; Samoc, M.; Samoc, A.; Zhu, L.-Y.; Yi, Y.-P.; Shuai, Z.-G. *J. Phys. Chem. A* **2007**, *111*, 472–478.

(17) Evans, I. P.; Spencer, A.; Wilkinson, G. *J. Chem. Soc., Dalton Trans.* **1973**, 204–209.

(18) Gillaizeau-Gauthier, I.; Odobel, F.; Alebbi, M.; Argazzi, R.; Costa, E.; Bignozzi, C. A.; Qu, P.; Meyer, G. J. *Inorg. Chem.* **2001**, *40*, 6073–6079.

(19) Maury, O.; Guégan, J.-P.; Renouard, T.; Hilton, A.; Dupau, P.; Sandon, N.; Toupet, L.; Le Bozec, H. *New J. Chem.* **2001**, *25*, 1553–1566.

(20) Coe, B. J.; Harris, J. A.; Asselberghs, I.; Clays, K.; Olbrechts, G.; Persoons, A.; Hupp, J. T.; Johnson, R. C.; Coles, S. J.; Hursthouse, M. B.; Nakatani, K. *Adv. Funct. Mater.* **2002**, *12*, 110–116.

(21) Coe, B. J.; Jones, L. A.; Harris, J. A.; Brunschwig, B. S.; Asselberghs, I.; Clays, K.; Persoons, A.; Garín, J.; Orduna, J. *J. Am. Chem. Soc.* **2004**, *126*, 3880–3891.

(22) Ichimura, K.; Watanabe, S. *J. Polym. Sci., Polym. Chem.* **1982**, *20*, 1419–1432.

C_5H_3N), 8.35 (4 H, d, $J = 6.5$ Hz, C_5H_4N), 8.14 (2 H, d, $J = 16.4$ Hz, CH), 7.90 (2 H, d, $J = 16.5$ Hz, CH), 7.80 (2 H, dd, $J = 5.2$, 1.4 Hz, C_5H_3N), 4.30 (6 H, s, Me). Anal. Calcd for $C_{26}H_{24}F_{12}N_4P_2 \cdot 0.8H_2O$: C, 44.81; H, 3.70; N, 8.04. Found: C, 44.79; H, 3.44; N, 8.10. ES-MS: *m/z* 537 ($[M - PF_6]^+$).

Synthesis of 4,4′-Bis{(*E*)-2-[*N*-(2,4-dinitrophenyl)-4-pyridyl] vinyl}-2,2′-bipyridyl Chloride, $[(2,4\text{-DNPh})_2bbpe^{2+}]Cl_2$. A mixture of bbpe·$0.5H_2O$ (300 mg, 0.808 mmol) and 2,4-dinitrochlorobenzene (1.81 g, 8.94 mmol) in ethanol (40 mL) was heated at reflux for 72 h, producing a beige precipitate. The precipitate was filtered off, washed with a small amount of ethanol and then dichloromethane and diethyl ether, and dried: yield 546 mg, 81%. ^{1}H NMR δ_H (CD_3SOCD_3): 9.38 (4 H, d, $J = 6.9$ Hz, C_5H_4N), 9.15 (2 H, d, $J = 2.6$ Hz, C_6H_3), 9.00 (2 H, dd, $J = 8.7$, 2.5 Hz, C_6H_3), 8.92 (2 H, d, $J = 5.0$ Hz, C_5H_3N), 8.83 (2 H, s, C_5H_3N), 8.67 (4 H, d, $J = 6.9$ Hz, C_5H_4N), 8.47−8.41 (4 H, C_6H_3 + CH), 8.11 (2 H, d, $J = 16.4$ Hz, CH), 7.89 (2 H, dd, $J = 5.0$, 1.3 Hz, C_5H_3N). Anal. Calcd for $C_{36}H_{24}Cl_2N_8O_8 \cdot 3.8H_2O$: C, 51.72; H, 3.81; N, 13.40. Found: C, 52.14; H, 3.62; N, 12.90. ES-MS: *m/z* 731 ($[M - Cl]^+$), 348 ($[M - 2Cl]^{2+}$).

Synthesis of 4,4′-Bis{(*E*)-2-[*N*-(2,4-dinitrophenyl)-4-pyridyl] vinyl}-2,2′-bipyridyl Hexafluorophosphate, $[(2,4\text{-DNPh})_2bbpe^{2+}][PF_6]_2$. $[(2,4\text{-DNPh})_2bbpe^{2+}]Cl_2 \cdot 3.8H_2O$ (536 mg, 0.641 mmol) was dissolved in a 1/1 methanol/water mixture. Slow addition of aqueous NH_4PF_6 (0.6 M) gave a beige precipitate, which was filtered off, washed with water, and dried: yield 570 mg, 89%. ^{1}H NMR δ_H (CD_3SOCD_3): 9.34 (4 H, d, $J = 6.7$ Hz, C_5H_4N), 9.15 (2 H, d, $J = 2.5$ Hz, C_6H_3), 9.00 (2 H, dd, $J = 8.7$, 2.4 Hz, C_6H_3), 8.92 (2 H, d, $J = 5.0$ Hz, C_5H_3N), 8.83 (2 H, s, C_5H_3N), 8.63 (4 H, d, $J = 6.6$ Hz, C_5H_4N), 8.43 (2 H, d, $J = 8.7$ Hz, C_6H_3), 8.38 (2 H, d, $J = 16.6$ Hz, CH), 8.07 (2 H, d, $J = 16.4$ Hz, CH), 7.87 (2 H, d, $J = 5.3$ Hz, C_5H_3N). Anal. Calcd for $C_{36}H_{24}F_{12}N_8O_8P_2 \cdot H_2O$: C, 43.04; H, 2.61; N, 11.15. Found: C, 43.24; H, 2.31; N, 10.96. ES-MS: *m/z* 841 ($[M - PF_6]^+$), 348 ($[M - 2PF_6]^{2+}$).

Synthesis of 4,4′-Bis[(*E*)-2-(*N*-phenyl-4-pyridyl)vinyl]-2,2′-bipyridyl Chloride, $[Ph_2bbpe^{2+}]Cl_2$. A mixture of 2,2′-bipyridyl-4,4′-dicarboxaldehyde (350 mg, 1.65 mmol) and $[Phpic^+]Cl \cdot 1.25H_2O$ (746 mg, 3.27 mmol) in acetic anhydride (20 mL) was heated at reflux in the dark for 1.5 h. The resulting beige precipitate was filtered off, washed with a small amount of acetic anhydride followed by acetone and then diethyl ether, and dried. Further purification was effected by reprecipitation from DMF/diethyl ether: yield 540 mg, 49%. ^{1}H NMR δ_H (CD_3SOCD_3): 9.37 (4 H, d, $J = 6.4$ Hz, C_5H_4N), 8.90 (2 H, d, $J = 5.0$ Hz, C_5H_3N), 8.80 (2 H, s, C_5H_3N), 8.56 (4 H, d, $J = 6.5$ Hz, C_5H_4N), 8.37 (2 H, d, $J = 16.2$ Hz, CH), 8.08 (2 H, d, $J = 16.4$ Hz, CH), 7.95−7.92 (4 H, m, Ph), 7.87 (2 H, d, $J = 5.8$ Hz, C_5H_3N), 7.80−7.72 (6 H, Ph). Anal. Calcd for $C_{36}H_{28}Cl_2N_4 \cdot 4.5H_2O$: C, 64.67; H, 5.58; N, 8.38. Found: C, 64.71; H, 5.46; N, 8.49. ES-MS: *m/z* 551 ($[M - Cl]^+$), 258 ($[M - 2Cl]^{2+}$).

Synthesis of 4,4′-Bis[(*E*)-2-(*N*-phenyl-4-pyridyl)vinyl]-2,2′-bipyridyl Hexafluorophosphate, $[Ph_2bbpe^{2+}][PF_6]_2$. $[Ph_2bbpe^{2+}]Cl_2 \cdot 4.5H_2O$ (540 mg, 0.808 mmol) was dissolved in methanol. Slow addition of aqueous NH_4PF_6 (0.6 M) gave a beige precipitate, which was filtered off, washed with water and then diethyl ether, and dried. Further purification was effected by reprecipitation from DMF/diethyl ether: yield 612 mg, 93%. ^{1}H NMR δ_H (CD_3SOCD_3): 9.35 (4 H, d, $J = 6.6$ Hz, C_5H_4N), 8.90 (2 H, d, $J = 4.9$ Hz, C_5H_3N), 8.81 (2 H, s, C_5H_3N), 8.53 (4 H, d, $J = 6.6$ Hz, C_5H_4N), 8.34 (2 H, d, $J = 16.7$ Hz, CH), 8.05 (2 H, d, $J = 16.5$ Hz, CH), 7.93−7.91 (4 H, m, Ph), 7.85 (2 H, d, $J = 4.4$ Hz, C_5H_3N), 7.80−7.74 (6 H, Ph). Anal. Calcd for $C_{36}H_{28}F_{12}N_4P_2 \cdot 0.6H_2O$: C, 52.90; H, 3.60; N, 6.85. Found: C, 52.90; H, 3.16; N, 6.85. ES-MS: *m/z* 661 ($[M - PF_6]^+$).

Synthesis of 4,4′-Bis[(*E*,*E*)-4-(4-pyridyl)buta-1,3-dienyl]-2,2′-bipyridyl, bbpb. This compound was prepared in a manner similar to that for bbpe by using potassium *tert*-butoxide (312 mg, 2.78 mmol), 4,4′-bis[(diethoxyphosphinyl)methyl]-2,2′-bipyridyl (500 mg, 1.10 mmol), and (*E*)-3-(4-pyridyl)-2-propenal (321 mg, 2.41 mmol) instead of 4-pyridinecarboxaldehyde. Distilled water (60 mL) was added and a cream-colored solid obtained: yield 325 mg, 70%. ^{1}H NMR δ_H ($CDCl_3$): 8.67 (2 H, d, $J = 5.5$ Hz, C_5H_3N), 8.59 (4 H, d, $J = 6.1$ Hz, C_5H_4N), 8.49 (2 H, s, C_5H_3N), 7.36−7.25 (8 H, C_5H_3N + C_5H_4N + CH), 7.16 (2 H, dd, $J = 15.2$, 10.8 Hz, CH), 6.80 (2 H, d, $J = 15.4$ Hz, CH), 6.72 (2 H, d, $J = 15.4$ Hz, CH). Anal. Calcd for $C_{28}H_{22}N_4 \cdot 0.5H_2O$: C, 79.41; H, 5.47; N, 13.23. Found: C, 79.43; H, 5.57; N, 12.79. EI-MS: *m/z* 415 (M^+).

Synthesis of 4,4′-Bis[(*E*,*E*)-4-(*N*-methyl-4-pyridyl)buta-1,3-dienyl]-2,2′-bipyridyl Iodide, $[Me_2bbpb^{2+}]I_2$. This compound was prepared in a manner similar to that for $[Me_2bbpe^{2+}]I_2$ by using bbpb·$0.5H_2O$ (200 mg, 0.472 mmol) instead of bbpe·$0.5H_2O$ and acetone (50 mL). Further purification was effected by precipitation from 1/1 DMF/diethyl ether to give an orange solid: yield 224 mg, 65%. ^{1}H NMR δ_H (CD_3SOCD_3): 8.87 (4 H, d, $J = 6.9$ Hz, C_5H_4N), 8.75 (2 H, d, $J = 5.1$ Hz, C_5H_3N), 8.54 (2 H, s, C_5H_3N), 8.21 (4 H, d, $J = 6.9$ Hz, C_5H_4N), 7.86 (2 H, dd, $J = 15.4$, 10.8 Hz, CH), 7.72 (2 H, dd, $J = 5.2$, 1.6 Hz, C_5H_3N), 7.62 (2 H, dd, $J = 15.5$, 10.8 Hz, CH), 7.19 (2 H, d, $J = 15.5$ Hz, CH), 7.12 (2 H, d, $J = 15.5$ Hz, CH), 4.26 (6 H, s, Me). Anal. Calcd for $C_{30}H_{28}I_2N_4 \cdot 1.9H_2O$: C, 49.18; H, 4.38; N, 7.65. Found: C, 49.17; H, 4.06; N, 7.56. ES-MS: *m/z* 571 ($[M - I]^+$).

Synthesis of 4,4′-Bis[(*E*,*E*)-4-(*N*-methyl-4-pyridyl)buta-1,3-dienyl]-2,2′-bipyridyl Hexafluorophosphate, $[Me_2bbpb^{2+}][PF_6]_2$. This compound was prepared in a manner similar to that for $[Me_2bbpe^{2+}][PF_6]_2$ by using $[Me_2bbpb^{2+}]I_2 \cdot 1.9H_2O$ (216 mg, 0.295 mmol) instead of $[Me_2bbpe^{2+}]I_2 \cdot 0.7H_2O$ in DMF (30 mL) to afford a bright yellow solid: yield 193 mg, 85%. ^{1}H NMR δ_H (CD_3SOCD_3): 8.86 (4 H, d, $J = 6.9$ Hz, C_5H_4N), 8.75 (2 H, d, $J = 5.1$ Hz, C_5H_3N), 8.55 (2 H, s, C_5H_3N), 8.20 (4 H, d, $J = 7.0$ Hz, C_5H_4N), 7.85 (2 H, dd, $J = 15.4$, 10.7 Hz, CH), 7.71 (2 H, dd, $J = 5.4$, 1.6 Hz, C_5H_3N), 7.62 (2 H, dd, $J = 15.5$, 10.7 Hz, CH), 7.18 (2 H, d, $J = 15.5$ Hz, CH), 7.11 (2 H, d, $J = 15.5$ Hz, CH), 4.26 (6 H, s, Me). Anal. Calcd for $C_{30}H_{28}F_{12}N_4P_2 \cdot 1.8H_2O$: C, 46.98; H, 4.15; N, 7.31. Found: C, 47.00; H, 3.83; N, 7.28. ES-MS: *m/z* 589 ($[M - PF_6]^+$).

Synthesis of 4,4′-Bis((*E*,*E*)-2-{4-[2-(4-pyridyl)vinyl]phenyl} vinyl)-2,2′-bipyridyl, bbpvb. This compound was prepared in a manner similar to that for bbpb by using 4-[(*E*)-2-(4-pyridyl)vinyl]benzaldehyde (515 mg, 2.45 mmol) instead of (*E*)-3-(4-pyridyl)-2-propenal in tetrahydrofuran (30 mL). Distilled water (40 mL) was added and a cream-colored solid obtained after an additional wash with ethyl acetate: yield 325 mg, 51%. ^{1}H NMR δ_H (CF_3CO_2D): 9.58 (2 H, d, $J = 6.4$ Hz, C_5H_3N), 9.31 (2 H, s, C_5H_3N), 9.27 (4 H, d, $J = 6.7$ Hz, C_5H_4N), 8.99 (2 H, d, $J = 6.4$ Hz, C_5H_3N), 8.78 (4 H, d, $J = 6.8$ Hz, C_5H_4N), 8.68 (2 H, d, $J = 16.2$ Hz, CH), 8.52−8.45 (10 H, C_6H_4 + CH), 8.17 (2 H, d, $J = 16.1$ Hz, CH), 8.07 (2 H, d, $J = 16.2$ Hz, CH). Anal. Calcd for $C_{40}H_{30}N_4 \cdot 0.5H_2O$: C, 83.45; H, 5.43; N, 9.73. Found: C, 83.47; H, 5.20; N, 9.63. EI-MS: *m/z* 567 (M^+).

Synthesis of 4,4′-Bis((*E*,*E*)-2-{4-[2-(*N*-methyl-4-pyridyl)vinyl]phenyl}-vinyl)-2,2′-bipyridyl Iodide, $[Me_2bbpvb^{2+}]I_2$. This compound was prepared in a manner similar to that for $[Me_2bbpb^{2+}]I_2$ by using bbpvb·$0.5H_2O$ (200 mg, 0.347 mmol) instead of bbpb·$0.5H_2O$ to afford an orange solid: yield 447 mg, 99%. ^{1}H NMR δ_H (CD_3SOCD_3): 8.87 (4 H, d, $J = 6.9$ Hz, C_5H_4N), 8.73 (2 H, d, $J = 5.1$ Hz, C_5H_3N), 8.61 (2 H, s, C_5H_3N), 8.23 (4 H, d, $J = 6.9$ Hz, C_5H_4N), 8.04 (2 H, d, $J = 16.2$ Hz, CH), 7.89−7.81 (8 H, m, C_6H_4), 7.73−7.68 (4 H, C_5H_3N + CH), 7.61−7.54 (4 H, CH), 4.26 (6 H, s, Me). Anal. Calcd for $C_{42}H_{36}I_2N_4 \cdot 2.5H_2O$: C, 56.33; H, 4.61; N, 6.26. Found: C, 56.31; H, 4.29; N, 6.17. ES-MS: *m/z* 723 ($[M - I]^+$).

Synthesis of 4,4′-Bis((*E*,*E*)-2-{4-[2-(*N*-methyl-4-pyridyl)vinyl] phenyl}vinyl)-2,2′-bipyridyl Hexafluorophosphate, $[Me_2bbpvb^{2+}][PF_6]_2$. This compound was prepared in a manner similar to that for $[Me_2bbpe^{2+}][PF_6]_2$ by using $[Me_2bbpvb^{2+}]I_2 \cdot 2.5H_2O$ (435 mg, 0.486 mmol) instead of $[Me_2bbpe^{2+}]I_2 \cdot 0.7H_2O$ in DMF (50 mL). Further purification was effected by precipitation from 1/1 DMF/diethyl ether to afford a bright yellow solid: yield 342 mg, 75%.

^{1}H NMR δ_H (CD_3SOCD_3): 8.86 (4 H, d, $J = 6.7$ Hz, C_5H_4N), 8.73 (2 H, d, $J = 5.1$ Hz, C_5H_3N), 8.61 (2 H, s, C_5H_3N), 8.22 (4 H, d, $J = 6.8$ Hz, C_5H_4N), 8.02 (2 H, d, $J = 16.3$ Hz, CH), 7.88−7.81 (8 H, m, C_6H_4), 7.72−7.68 (4 H, C_5H_3N + CH), 7.60−7.54 (4 H, CH), 4.26 (6 H, s, Me). Anal. Calcd for $C_{42}H_{36}F_{12}N_4P_2 \cdot 2.8H_2O$: C, 53.83; H, 4.47; N, 5.98. Found: C, 53.80; H, 3.94; N, 5.97. ES-MS: m/z 741 ($[M - PF_6]^+$).

Synthesis of $[Ru^{II}(Me_2bbpe^{2+})_3][PF_6]_8$, 2. A mixture of *cis*-$Ru^{II}Cl_2(DMSO)_4$ (33 mg, 0.068 mmol), silver(I) tosylate (38 mg, 0.136 mmol), and $[Me_2bbpe^{2+}][PF_6]_2 \cdot 0.8H_2O$ (162 mg, 0.232 mmol) in degassed DMF (10 mL) was heated at reflux for 4 h under Ar in the dark. The resulting red mixture was cooled to room temperature, and the AgCl precipitate was filtered off. Addition of aqueous NH_4PF_6 to the filtrate produced a red precipitate, which was filtered off, washed with water, and dried. The crude product was dissolved in acetonitrile solution, loaded onto a silica gel column (230−400 mesh, 5 × 22 cm), and eluted with 0.1 M NH_4PF_6 in acetonitrile, giving a major dark red band. Fractions were collected and compared by TLC. Similar fractions were combined, reduced to dryness, and precipitated from acetone/aqueous NH_4PF_6 to afford a dark red-brown solid: 83 mg, 49%. ^{1}H NMR δ_H (CD_3CN): 8.88 (6 H, d, $J = 1.3$ Hz, C_5H_3N), 8.59 (12 H, d, $J = 6.8$ Hz, C_5H_4N), 8.13 (12 H, d, $J = 6.9$ Hz, C_5H_4N), 7.90−7.79 (18 H, CH + C_5H_3N), 7.65 (6 H, dd, $J = 6.0$, 1.7 Hz, C_5H_3N), 4.27 (18 H, s, Me). Anal. Calcd for $C_{78}H_{72}F_{48}N_{12}P_8Ru \cdot 3.5H_2O$: C, 37.45; H, 3.18; N, 6.72. Found: C, 37.44; H, 2.91; N, 6.73.

Synthesis of $[Ru^{II}(Me_2bbpe^{2+})_3][BPh_4]_7PF_6$, 2B. A portion of **2** (19 mg, 7.60 μmol) in acetone (2 mL) was treated with aqueous $NaBPh_4$, and the dark red precipitate was filtered off, washed with water, and dried: yield 22 mg, 79%. ^{1}H NMR δ_H (CD_3SOCD_3): 9.23 (6 H, s, C_5H_3N), 8.89 (12 H, d, $J = 6.4$ Hz, C_5H_4N), 8.16 (12 H, d, $J = 6.0$ Hz, C_5H_4N), 7.99 (6 H, d, $J = 16.4$ Hz, CH), 7.93 (6 H, d, $J = 16.4$ Hz, CH), 7.86 (6 H, d, $J = 6.0$ Hz, C_5H_3N), 7.51 (6 H, d, $J = 6.0$, C_5H_3N), 7.24−7.10 (56 H, m, Ph), 6.95−6.84 (56 H, m, Ph), 6.80−6.70 (28 H, m, Ph), 4.27 (18 H, s, Me). Anal. Calcd for $C_{246}H_{212}B_7F_6N_{12}PRu$: C, 80.77; H, 5.84; N, 4.59. Found: C, 80.70; H, 5.76; N, 4.29.

Synthesis of $[Ru^{II}(Ph_2bbpe^{2+})_3][PF_6]_8$, 4. This compound was prepared and purified in a manner similar to that for **2** by using $[Ph_2bbpe^{2+}][PF_6]_2 \cdot 0.6H_2O$ (192 mg, 0.235 mmol) instead of $[Me_2bbpe^{2+}][PF_6]_2 \cdot 0.8H_2O$ to afford a dark orange-red solid: yield 124 mg, 63%. ^{1}H NMR δ_H (CD_3CN): 9.00 (6 H, d, $J = 1.2$ Hz, C_5H_3N), 8.92 (12 H, d, $J = 7.1$ Hz, C_5H_4N), 8.34 (12 H, d, $J = 7.1$ Hz, C_5H_4N), 8.10−7.90 (18 H, CH + C_5H_3N), 7.77−7.72 (36 H, C_5H_3N + Ph). Anal. Calcd for $C_{108}H_{84}F_{48}N_{12}P_8Ru \cdot 4.3H_2O$: C, 44.91; H, 3.23; N, 5.82. Found: C, 44.91; H, 2.94; N, 5.74.

Synthesis of $[Ru^{II}(Me_2bbpb^{2+})_3][PF_6]_8$, 5. This compound was prepared and purified in a manner similar to that for **2** by using $[Me_2bbpb^{2+}][PF_6]_2 \cdot 1.8H_2O$ (175 mg, 0.228 mmol) instead of $[Me_2bbpe^{2+}][PF_6]_2 \cdot 0.8H_2O$ to afford a dark orange-red solid: yield 92 mg, 51%. ^{1}H NMR δ_H (CD_3CN): 8.70 (6 H, d, $J = 1.4$ Hz, C_5H_3N), 8.48 (12 H, d, $J = 6.9$ Hz, C_5H_4N), 7.99 (12 H, d, $J = 6.9$ Hz, C_5H_4N), 7.74 (6 H, d, $J = 6.1$ Hz, C_5H_3N), 7.70−7.59 (12 H, CH), 7.54 (6 H, dd, $J = 6.1$, 1.6 Hz, C_5H_3N), 7.16 (6 H, d, $J = 14.8$ Hz, CH), 7.05 (6 H, d, $J = 14.8$ Hz, CH), 4.22 (18 H, s, Me). Anal. Calcd for $C_{90}H_{84}F_{48}N_{12}P_8Ru \cdot 4.3H_2O$: C, 40.46; H, 3.49; N, 6.29. Found: C, 40.46; H, 3.01; N, 6.24.

Synthesis of $[Ru^{II}(Me_2bbpvb^{2+})_3][PF_6]_8$, 6. This compound was prepared and purified in a manner similar to that for **2** by using *cis*-$Ru^{II}Cl_2(DMSO)_4$ (28 mg, 0.058 mmol), silver(I) tosylate (33 mg, 0.118 mmol), and $[Me_2bbpvb^{2+}][PF_6]_2 \cdot 2.8H_2O$ (180 mg, 0.203 mmol) to afford a dark red solid: yield 134 mg, 75%. ^{1}H NMR δ_H (CD_3CN): 8.80 (6 H, d, $J = 1.5$ Hz, C_5H_3N), 8.47 (12 H, d, $J = 7.0$ Hz, C_5H_4N), 8.02 (12 H, d, $J = 7.0$ Hz, C_5H_4N), 7.86−7.77 (42 H, C_5H_3N + C_6H_4 + CH), 7.57 (6 H, dd, $J = 6.1$, 1.5 Hz, C_5H_3N), 7.48−7.40 (12 H, CH), 4.21 (18 H, s, Me). Anal. Calcd for $C_{126}H_{108}F_{48}N_{12}P_8Ru \cdot 2.3H_2O$: C, 48.94; H, 3.67; N, 5.44. Found: C, 48.93; H, 3.56; N, 5.28.

Synthesis of $[Fe^{II}(Me_2bbpe^{2+})_3][PF_6]_8$, 8. $Fe^{II}(BF_4)_2 \cdot 6H_2O$ (20 mg, 0.059 mmol) was added to a solution of $[Me_2bbpe^{2+}][PF_6]_2 \cdot 0.8H_2O$ (129 mg, 0.185 mmol) in DMF (10 mL), and the deep blue solution was stirred at room temperature for 2 h in the dark. Addition of aqueous NH_4PF_6 afforded a dark blue precipitate, which was filtered off, washed with water, and dried. Purification was effected as for **2** to afford a dark blue solid: yield 90 mg, 62%. ^{1}H NMR δ_H (CD_3CN): 8.90 (6 H, d, $J = 1.4$ Hz, C_5H_3N), 8.59 (12 H, d, $J = 6.9$ Hz, C_5H_4N), 8.14 (12 H, d, $J = 7.0$ Hz, C_5H_4N), 7.89 (6 H, d, $J = 16.5$ Hz, CH), 7.83 (6 H, d, $J = 16.5$ Hz, CH), 7.64 (6 H, dd, $J = 6.1$, 1.8 Hz, C_5H_3N), 7.57 (6 H, d, $J = 6.0$ Hz, C_5H_3N), 4.29 (18 H, s, Me). Anal. Calcd for $C_{78}H_{72}F_{48}FeN_{12}P_8 \cdot 3.5H_2O$: C, 38.14; H, 3.24; N, 6.84. Found: C, 38.13; H, 2.89; N, 6.80.

Synthesis of $[Fe^{II}(Me_2bbpe^{2+})_3][BPh_4]_{7.3}[PF_6]_{0.7}$, 8B. This compound was prepared in a manner similar to that for **2B** by using **8** (47 mg, 19.1 μmol) instead of **2** to afford a dark blue solid: yield 63 mg, 90%. ^{1}H NMR δ_H (CD_3CN): 8.28 (6 H, s, C_5H_3N), 8.25 (12 H, d, $J = 6.8$ Hz, C_5H_4N), 7.68 (12 H, d, $J = 6.8$ Hz, C_5H_4N), 7.36 (6 H, d, $J = 16.4$ Hz, CH), 7.25−7.19 (70.4 H, C_5H_3N + CH + Ph), 6.97 (6 H, dd, $J = 6.2$, 1.5 Hz, C_5H_3N), 6.91−6.88 (58.4 H, m, Ph), 6.80−6.76 (29.2 H, m, Ph), 4.13 (18 H, s, Me). Anal. Calcd for $C_{253.2}H_{218}B_{7.3}F_{4.2}FeN_{12}P_{0.7}$: C, 82.97; H, 6.00; N, 4.59. Found: C, 82.89; H, 6.02; N, 4.47.

Synthesis of $[Fe^{II}(Ph_2bbpe^{2+})_3][PF_6]_8$, 10. This compound was prepared and purified in a manner similar to that for **8** by using $[Ph_2bbpe^{2+}][PF_6]_2 \cdot 0.6H_2O$ (153 mg, 0.187 mmol) instead of $[Me_2bbpe^{2+}][PF_6]_2 \cdot 0.8H_2O$ to afford a dark blue solid: yield 121 mg, 73%. ^{1}H NMR δ_H (CD_3CN): 9.01 (6 H, d, $J = 1.4$ Hz, C_5H_3N), 8.92 (12 H, d, $J = 7.1$ Hz, C_5H_4N), 8.34 (12 H, d, $J = 7.1$ Hz, C_5H_4N), 8.05 (6 H, d, $J = 16.5$ Hz, CH), 7.98 (6 H, d, $J = 16.5$ Hz, CH), 7.77−7.71 (36 H, C_5H_3N + Ph), 7.65 (6 H, d, $J = 6.0$ Hz, C_5H_3N). Anal. Calcd for $C_{108}H_{84}F_{48}FeN_{12}P_8 \cdot 2H_2O$: C, 46.30; H, 3.17; N, 6.00. Found: C, 46.27; H, 2.91; N, 5.98.

Synthesis of $[Fe^{II}(Me_2bbpb^{2+})_3][PF_6]_8$, 11. This compound was prepared and purified in a manner similar to that for **8** by using $[Me_2bbpb^{2+}][PF_6]_2 \cdot 1.8H_2O$ (131 mg, 0.171 mmol) instead of $[Me_2bbpe^{2+}][PF_6]_2 \cdot 0.8H_2O$ to afford a dark blue solid: yield 85 mg, 57%. ^{1}H NMR δ_H (CD_3CN): 8.72 (6 H, d, $J = 1.2$ Hz, C_5H_3N), 8.48 (12 H, d, $J = 6.8$ Hz, C_5H_4N), 8.00 (12 H, d, $J = 6.8$ Hz, C_5H_4N), 7.71−7.61 (12 H, CH), 7.52 (6 H, dd, $J = 6.0$, 1.5 Hz, C_5H_3N), 7.43 (6 H, d, $J = 6.1$ Hz, C_5H_3N), 7.20−7.13 (6 H, m, CH), 7.09−7.02 (6 H, m, CH), 4.22 (18 H, s, Me). Anal. Calcd for $C_{90}H_{84}F_{48}FeN_{12}P_8 \cdot 4.2H_2O$: C, 41.18; H, 3.55; N, 6.40. Found: C, 41.17; H, 3.24; N, 6.26.

Synthesis of $[Fe^{II}\{(2,4\text{-}DNPh)_2bbpe^{2+}\}_3][PF_6]_8$, 12. This compound was prepared in a manner similar to that for **8** by using $[(2,4\text{-}DNPh)_2bbpe^{2+}][PF_6]_2 \cdot H_2O$ (175 mg, 0.174 mmol) instead of $[Me_2bbpe^{2+}][PF_6]_2 \cdot 0.8H_2O$. Purification was achieved by careful reprecipitation from acetone/ethanol to afford a dark blue solid: yield 185 mg, 94%. ^{1}H NMR δ_H (CD_3CN): 9.17 (6 H, d, $J = 2.5$ Hz, C_6H_3), 9.03 (6 H, d, $J = 1.5$ Hz, C_5H_3N), 8.85−8.82 (18 H, C_6H_3 + C_5H_4N), 8.41 (12 H, d, $J = 7.0$ Hz, C_5H_4N), 8.14−8.00 (12 H, C_6H_3 + CH), 8.01 (6 H, d, $J = 16.4$ Hz, CH), 7.75 (6 H, dd, $J = 5.8$, 1.4 Hz, C_5H_3N), 7.69 (6 H, d, $J = 6.0$ Hz, C_5H_3N). Anal. Calcd for $C_{108}H_{72}F_{48}FeN_{24}O_{24}P_8 \cdot 4.2H_2O$: C, 38.37; H, 2.40; N, 9.94. Found: C, 38.35; H, 1.97; N, 9.88.

Synthesis of $[Fe^{II}\{(2,4\text{-}DNPh)_2bbpe^{2+}\}_3][BPh_4]_{6.55}[PF_6]_{1.45}$, 12B. This compound was prepared in a manner similar to that for **2B** by using **12** (31 mg, 9.17 μmol) instead of **2** to afford a dark blue solid: yield 25 mg, 61%. ^{1}H NMR δ_H (CD_3CN): 9.15 (6 H, d, $J = 2.4$ Hz, C_6H_3), 8.76 (6 H, dd, $J = 8.8$, 2.4 Hz, C_6H_3), 8.37−8.32 (18 H, C_6H_3 + C_5H_4N), 7.87−7.82 (18 H, C_5H_4N + C_5H_3N), 7.52 (6 H, d, $J = 16.4$ Hz, CH), 7.36−7.21 (64.4 H, C_6H_3N + CH + Ph), 7.05 (6 H, dd, $J = 5.8$, 1.6 Hz, C_5H_3N), 6.94−6.86 (52.4 H, Ph), 6.81−6.74 (26.2 H, Ph). Anal. Calcd for $C_{265.2}H_{203}B_{6.55}F_{8.7}FeN_{24}O_{24}P_{1.45}$: C, 71.63; H, 4.60; N, 7.56. Found: C, 71.63; H, 4.58; N, 7.05.

Table 1. Crystallographic Data and Refinement Details for the Salt $[Ph_2bbpe^{2+}][PF_6]_2 \cdot 2DMF$

formula	$C_{42}H_{42}F_{12}N_6O_2P_2$
M	952.76
cryst syst	monoclinic
space group	$P2_1/c$
a, Å	9.1252(13)
b, Å	17.637(2)
c, Å	13.683(2)
β, deg	109.478(5)
V, Å^3	2076.1(5)
Z	2
T, K	100(2)
μ, mm^{-1}	0.205
cryst size, mm^3	0.30 × 0.25 × 0.20
cryst appearance	pale brown prism
no. of rflns collected	11 919
no. of indep rflns (R_{int})	4694 (0.0315)
no. of rflns with $I > 2\sigma(I)$	3259
goodness of fit on F^2	1.123
final R1, wR2 ($I > 2\sigma(I)$)[a]	0.0561, 0.1595
(all data)	0.0802, 0.1736
peak and hole, e Å^{-3}	0.853, −0.569

[a] The structure was refined on F_o^2 using all data; the values of R1 are given for comparison with older refinements based on F_o with a typical threshold of $F_o > 4\sigma(F_o)$.

Synthesis of $[Fe^{II}(Me_2bbpvb^{2+})_3][PF_6]_8$, 13. This compound was prepared and purified in a manner similar to that for **8** by using $[Me_2bbpvb^{2+}][PF_6]_2 \cdot 2.8H_2O$ (131 mg, 0.140 mmol) instead of $[Me_2bbpe^{2+}][PF_6]_2 \cdot 0.8H_2O$. A final reprecipitation from acetonitrile/diethyl ether afforded a dark blue solid: yield 107 mg, 75%. ^{1}H NMR δ_H (CD_3CN): 8.83 (6 H, d, J = 1.4 Hz, C_5H_3N), 8.47 (12 H, d, J = 6.9 Hz, C_5H_4N), 8.02 (12 H, d, J = 7.0 Hz, C_5H_4N), 7.86−7.81 (36 H, $C_5H_3N + C_6H_4 +$ CH), 7.56 (6 H, dd, J = 6.1, 1.5 Hz, C_5H_3N), 7.50−7.40 (18 H, CH), 4.21 (18 H, s, Me). Anal. Calcd for $C_{126}H_{108}F_{48}FeN_{12}P_8 \cdot 3.4H_2O$: C, 49.34; H, 3.77; N, 5.48. Found: C, 49.32; H, 3.55; N, 5.52.

X-ray Crystallography. Crystals of the proligand salt $[Ph_2bbpe^{2+}][PF_6]_2 \cdot 2DMF$ were obtained by slow diffusion of diethyl ether vapor into a DMF solution. Data were collected on an Oxford Diffraction XCalibur 2 X-ray diffractometer and processed (including absorption correction) using the Oxford Diffraction CrysAlis RED software package,[23] before final ins and *hkl* files were prepared using the SHELXTL program suite.[24] The structure was solved by direct methods using SIR-92[25] via WinGX[26] and refined by full-matrix least squares on all F_o^2 values using SHELXL-97[27] via SHELXTL. All non-hydrogen atoms were refined anisotropically, and hydrogen atoms were included in idealized positions using the riding model, with thermal parameters 1.2 times those of aryl parent carbon atoms and 1.5 times those of methyl parent carbons. The asymmetric unit contains half of one Ph_2bbpe^{2+} dication, one PF_6^- anion, and one DMF molecule. All other calculations were carried out using the SHELXTL package.[24] Crystallographic data and refinement details are presented in Table 1.

Hyper-Rayleigh Scattering. Details of the hyper-Rayleigh scattering (HRS) experiment have been discussed elsewhere,[28] and the experimental procedure used for the nanosecond measurements was as previously described.[29] The latter studies were performed by using the 1064 nm fundamental of an injection-seeded, Q-switched Nd:YAG laser (Quanta-Ray PRO, 8 ns pulses, 7 mJ, 10 Hz). β values were determined by using the electric-field-induced second harmonic generation $\beta_{zzz,1064}$ for *p*-nitroaniline (29×10^{-30} esu in acetonitrile)[30] as an external reference. The different nature of the reference tensor component for *p*-nitroaniline has been taken into account in deriving the octupolar β_{xxx} values for the compounds studied. The apparatus and experimental procedures used for the femtosecond HRS studies were exactly as described previously.[31] These measurements were also carried out in acetonitrile, and the reference compound was crystal violet (octupolar $\beta_{xxx,800} = 327 \times 10^{-30}$ esu in acetonitrile; from the value of 338×10^{-30} esu in methanol, corrected for local field factors at optical frequencies). For all measurements, dilute solutions (10^{-5}−10^{-6} M) were used to ensure a linear dependence of $I_{2\omega}/I_\omega^2$ on concentration, precluding the need for Lambert−Beer correction factors. The absence of demodulation at 800 nm, i.e. constant values of β versus frequency, confirmed that no luminescence contributions to the HRS signals were present at 400 nm, consistent with the observation of luminescence well above this wavelength (for the Ru compounds) or no luminescence at all (for the Fe compounds). The reported $\beta_{xxx,800}$ values are the averages taken from measurements at different amplitude modulation frequencies.

Stark Spectroscopy. The Stark apparatus, experimental methods, and data collection procedure were as previously reported,[32] except that a Xe arc lamp was used as the light source in the place of a W filament bulb. The Stark spectrum for each compound was measured at least twice. To fit the Stark data, the absorption (ε/ν vs ν) spectrum was modeled with a sum of Gaussian curves that reproduce the data and separate the peaks. The first and second derivatives of the Gaussian curves were then used to fit the Stark spectra with Liptay's equation.[33] The dipole moment change, $\Delta\mu_{12} = \mu_e - \mu_g$, where μ_e and μ_g are the respective excited- and ground-state dipole moments, associated with each of the optical transitions considered in the fit was then calculated from the coefficient of the second-derivative component. Butyronitrile was used as the glassing medium, for which the local field correction f_{int} is estimated as 1.33.[32] A two-state analysis of the ICT transitions gives

$$\Delta\mu_{ab}^2 = \Delta\mu_{12}^2 + 4\mu_{12}^2 \quad (1)$$

where $\Delta\mu_{ab}$ is the dipole moment change between the diabatic states and $\Delta\mu_{12}$ is the observed (adiabatic) dipole moment change. The value of the transition dipole moment μ_{12} can be determined from the oscillator strength f_{os} of the transition by

(23) CrysAlis RED (Version 1.171.32.4); Oxford Diffraction Ltd., Yarnton, Oxfordshire, U.K., 2006.
(24) SHELXTL (Version 6.10); Bruker AXS Inc., Madison, WI, 2000.
(25) Altomare, A.; Cascarano, G.; Giacovazzo, C.; Guagliardi, A.; Burla, M. C.; Polidori, G.; Camalli, M. *J. Appl. Crystallogr.* **1994**, *27*, 435–435.
(26) Farrugia, L. J. *J. Appl. Crystallogr.* **1999**, *32*, 837–838.
(27) Sheldrick, G. M. SHELXL 97, Programs for Crystal Structure Analysis (Release 97-2); University of Göttingen, Göttingen, Germany, 1997.
(28) (a) Terhune, R. W.; Maker, P. D.; Savage, C. M. *Phys. Rev. Lett.* **1965**, *14*, 681–684. (b) Clays, K.; Persoons, A. *Phys. Rev. Lett.* **1991**, *66*, 2980–2983. (c) Clays, K.; Persoons, A. *Rev. Sci. Instrum.* **1992**, *63*, 3285–3289. (d) Hendrickx, E.; Clays, K.; Persoons, A. *Acc. Chem. Res.* **1998**, *31*, 675–683.
(29) Houbrechts, S.; Clays, K.; Persoons, A.; Pikramenou, Z.; Lehn, J.-M. *Chem. Phys. Lett.* **1996**, *258*, 485–489.
(30) Stähelin, M.; Burland, D. M.; Rice, J. E. *Chem. Phys. Lett.* **1992**, *191*, 245–250.
(31) (a) Olbrechts, G.; Strobbe, R.; Clays, K.; Persoons, A. *Rev. Sci. Instrum.* **1998**, *69*, 2233–2244. (b) Olbrechts, G.; Wostyn, K.; Clays, K.; Persoons, A. *Opt. Lett.* **1999**, *24*, 403–405. (c) Clays, K.; Wostyn, K.; Olbrechts, G.; Persoons, A.; Watanabe, A.; Nogi, K.; Duan, X.-M.; Okada, S.; Oikawa, H.; Nakanishi, H.; Vogel, H.; Beljonne, D.; Brédas, J.-L. *J. Opt. Soc. Am. B* **2000**, *17*, 256–265. (d) Franz, E.; Harper, E. C.; Coe, B. J.; Zahradnik, P.; Clays, K.; Asselberghs, I. *Proc. SPIE-Int. Soc. Opt. Eng.* **2008**, *6999*, 699923-1–699923-11.
(32) (a) Shin, Y. K.; Brunschwig, B. S.; Creutz, C.; Sutin, N. *J. Phys. Chem.* **1996**, *100*, 8157–8169. (b) Coe, B. J.; Harris, J. A.; Brunschwig, B. S. *J. Phys. Chem. A* **2002**, *106*, 897–905.
(33) (a) Liptay, W. In *Excited States*; Lim, E. C., Ed.; Academic Press: New York, 1974; Vol. 1, pp 129−229. (b) Bublitz, G. U.; Boxer, S. G. *Annu. Rev. Phys. Chem.* **1997**, *48*, 213–242. (c) Vance, F. W.; Williams, R. D.; Hupp, J. T. *Int. Rev. Phys. Chem.* **1998**, *17*, 307–329. (d) Brunschwig, B. S.; Creutz, C.; Sutin, N. *Coord. Chem. Rev.* **1998**, *177*, 61–79.

$$|\mu_{12}| = \left(\frac{f_{os}}{1.08 \times 10^{-5} E_{max}}\right)^{1/2} \quad (2)$$

where E_{max} is the energy of the ICT maximum (in wavenumbers) and μ_{12} is in eÅ. The latter is converted into Debye units upon multiplying by 4.803. The degree of delocalization c_b^2 and electronic coupling matrix element H_{ab} for the diabatic states are given by

$$c_b^2 = \frac{1}{2}\left[1 - \left(\frac{\Delta\mu_{12}^2}{\Delta\mu_{12}^2 + 4\mu_{12}^2}\right)^{1/2}\right] \quad (3)$$

$$|H_{ab}| = \left|\frac{E_{max}(\mu_{12})}{\Delta\mu_{ab}}\right| \quad (4)$$

If the hyperpolarizability β_0 tensor has only nonzero elements along the ICT direction, then this quantity is given by

$$\beta_0 = \frac{3\Delta\mu_{12}(\mu_{12})^2}{(E_{max})^2} \quad (5)$$

A relative error of ±20% is estimated for the β_0 values derived from the Stark data and using eq 5, while experimental errors of ±10% are estimated for μ_{12}, $\Delta\mu_{12}$, and $\Delta\mu_{ab}$, ±15% for H_{ab}, and ±50% for c_b^2.

Z-Scan Measurements. All compounds were investigated as DMF solutions placed in 1 mm path length glass cells. The measurements were carried out at 750 nm (1.652 eV). This wavelength was chosen in such a way as to provide the optimum possible enhancement of the NLO properties of the compounds while avoiding excessive one-photon absorption. The system used for the measurements used a Clark-MXR regenerative amplifier operating at 250 Hz and generating ca. 800 μJ pulses at 775 nm, which were used to pump a Light Conversion TOPAS traveling wave optical parametric amplifier (OPA). The wavelength for the present measurements was obtained by doubling the OPA signal.

A standard Z-scan measurement system was used, the beam from the OPA being first attenuated and spatially filtered by a pair of apertures and then focused with a lens to form a $w_0 \approx 60$ μm spot at the focal plane: i.e., $z = 0$. The cell was mounted on a traveling stage which was moved from $z = -40$ to $z = 40$ mm. The beam transmitted through the sample was probed with a beam splitter to provide an "open aperture" signal and with an iris aperture in the far field to provide the "closed aperture" signal simultaneously. The Z-scans were analyzed using home-written software implementing the calculations as presented by Sheikh-Bahae et al.[34]

By comparing the shapes of computed curves with the experimental ones, we obtained the values of the nonlinear phase shift $\Delta\Phi_0$ (=Re($\Delta\hat{\Phi}_0$)) and the T factor defined here according to the equation

$$T = 4\pi\frac{\mathrm{Im}(\Delta\hat{\Phi}_0)}{\mathrm{Re}(\Delta\hat{\Phi}_0)} \quad (6)$$

where $\Delta\hat{\Phi}_0$ stands for the complex phase shift. All measurements were performed in the range of intensities at which the phase shifts were below ca. 1 rad. The Z-scans were measured for three concentrations of each compound in DMF (the highest concentration being typically about 4 wt %) as well as for the solvent itself, and the real and imaginary components of the γ response of the solute were determined assuming linear dependences of the real and imaginary parts of the phase shift on concentration as described elsewhere.[35] The data were calibrated against the nonlinearity of fused silica, which was taken to be $n_2 = 2.78 \times 10^{-16}$ cm^2 W^{-1} at 750 nm.[35] The nonlinear absorption was also expressed in terms of the values of σ_2 calculated as shown previously.[35]

Results and Discussion

Synthetic Studies. The new 4,4′-disubstituted bpy derivatives bbpe, bbpb, and bbpvb were prepared in good yields via Wadsworth−Emmons reactions of 4,4′-bis-[(diethoxyphosphinyl)methyl]-2,2′-bipyridyl with the appropriate aldehyde in THF at room temperature using potassium *tert*-butoxide as the base (Scheme 1a). Although the related compound 4-methyl-4′-[(*E*)-2-(4-pyridyl)vinyl]-2,2′-bipyridyl is already known,[36] perhaps surprisingly, to our knowledge bbpe has not been reported previously. Dimethylation of bbpe, bbpb, and bbpvb with iodomethane in acetone proceeded smoothly to afford the salts [Me$_2$bbpe^{2+}]I$_2$, [Me$_2$bbpb^{2+}]I$_2$, and [Me$_2$bbpvb^{2+}]I$_2$, with no evidence for methylation of the bpy N atoms. The salt [(2,4-DNPh)$_2$bbpe^{2+}]Cl$_2$ was prepared in high yield via reaction of bbpe with an excess of 2,4-dinitrochlorobenzene in ethanol under reflux (Scheme 1a), as previously described for the preparation of [(2,4-DNPh)$_2$qpy^{2+}]Cl$_2$ (qpy = 2,2′:4,4″:4′,4‴-quaterpyridyl).[15] We have previously used a Zincke-type reaction with aniline to convert (2,4-DNPh)$_2$qpy^{2+} into Ph$_2$qpy^{2+}.[37] However, attempts at achieving a similar reaction of [(2,4-DNPh)$_2$bbpe^{2+}]Cl$_2$ under various different conditions failed to yield any trace of [Ph$_2$bbpe^{2+}]Cl$_2$. We therefore prepared the latter compound in good yield by a Knoevenagel-type reaction of [Phpic$^+$]Cl with 2,2′-bipyridyl-4,4′-dicarboxaldehyde using acetic anhydride as the solvent and dehydration catalyst (Scheme 1b). All of the new proligand halide salts were readily converted into their corresponding hexafluorophosphate salts by anion metathesis with aqueous NH_4PF_6.

The Ru^{II} complex salts **2** and **4**−**6** (Figure 1) were prepared via a previously reported procedure[15] involving reactions of the precursor *cis*-Ru^{II}Cl$_2$(DMSO)$_4$[17] with [Me$_2$bbpe^{2+}][PF$_6$]$_2$, [Me$_2$bbpb^{2+}][PF$_6$]$_2$, [Me$_2$bbpvb^{2+}][PF$_6$]$_2$, or [Ph$_2$bbpe^{2+}][PF$_6$]$_2$. Yields of ca. 50−65% were obtained after column chromatographic purification. Attempts to isolate the compound [Ru^{II}{(2,4-DNPh)$_2$bbpe^{2+}}$_3$][PF$_6$]$_8$ were unfortunately unsuccessful, probably due to decomposition of the strongly electron-deficient pyridinium units under the relatively harsh reaction conditions used (DMF under reflux). However, the use of milder conditions (DMF at room temperature) and the precursor Fe^{II}(BF$_4$)$_2$·6H$_2$O allowed the synthesis of [Fe^{II}{(2,4-DNPh)$_2$bbpe^{2+}}$_3$][PF$_6$]$_8$ (**12**) as well as the other related Fe^{II} complex salts **8**, **10**, **11**, and **13** (Figure 1). The last four compounds were purified by using column chromatography and isolated in yields of ca. 55−75%, while **12** was obtained pure in over 90% yield without any need for chromatographic purification.

The expected *E* configuration of the ethenyl units in all of the proligands and complex salts is confirmed by the ^{1}H NMR coupling constants J in the range ca. 15−17 Hz in all cases (except where signal overlap prevents these from being measured). The alternative *Z* configuration would give J values of

(34) (a) Sheik-Bahae, M.; Said, A. A.; van Stryland, E. W. *Opt. Lett.* **1989**, *14*, 955–957. (b) Sheik-Bahae, M.; Said, A. A.; Wei, T. H.; Hagan, D. J.; van Stryland, E. W. *IEEE J. Quantum Electron.* **1990**, *26*, 760–769. (c) van Stryland, E. W.; Sheik-Bahae, M. *Opt. Eng.* **1998**, *60*, 655–692.

(35) Samoc, M.; Samoc, A.; Dalton, G. T.; Cifuentes, M. P.; Humphrey, M. G.; Fleitz, P. A. In *Multiphoton Processes in Organics and Their Application*; Rau, I., Kajzar, F., Eds.; Old City Publishing: Philadelphia, in press.

(36) Kim, D.; Shin, E. J. *Bull. Korean Chem. Soc.* **2003**, *24*, 1490–1494.

(37) Coe, B. J.; Harris, J. A.; Jones, L. A.; Brunschwig, B. S.; Song, K.; Clays, K.; Garín, J.; Orduna, J.; Coles, S. J.; Hursthouse, M. B. *J. Am. Chem. Soc.* **2005**, *127*, 4845–4859.

Scheme 1. Syntheses of the New Proligand Salts $[Me_2bbpe^{2+}][PF_6]_2$, $[Me_2bbpb^{2+}][PF_6]_2$, $[Me_2bbpvb^{2+}][PF_6]_2$, $[(2,4\text{-}DNPh)_2bbpe^{2+}][PF_6]_2$, and $[Ph_2bbpe^{2+}][PF_6]_2$, Together with Their Precursors bbpe, bbpb, and bbpvb[a]

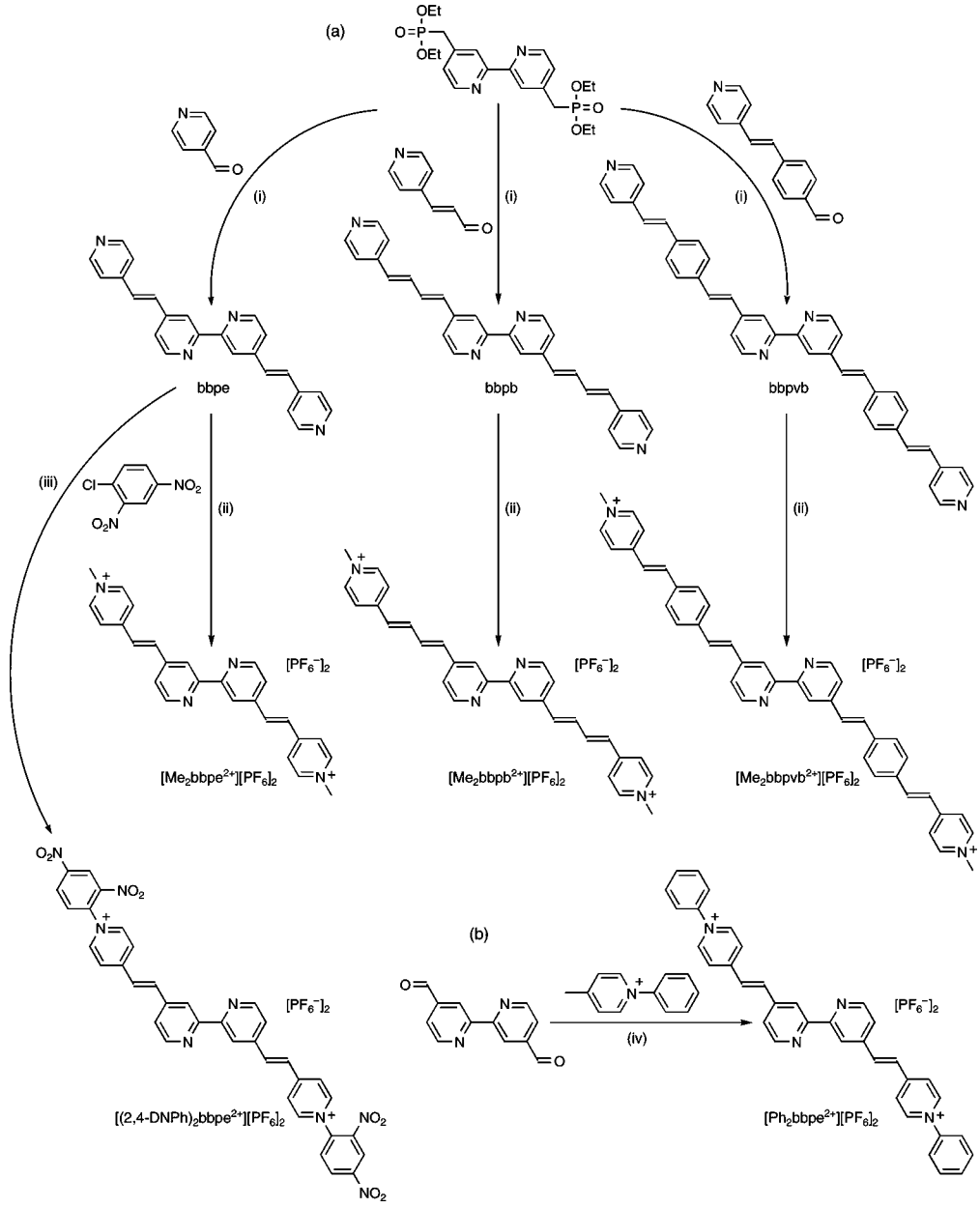

[a] Legend: (i) KO^{t}Bu/THF; (ii) MeI/Me_2CO, then NH_4PF_6; (iii) EtOH under reflux, then NH_4PF_6; (iv) Ac_2O under reflux, then NH_4PF_6.

about 11 Hz and also doublets shifted to relatively higher fields. We have observed no evidence for thermal isomerization/photoisomerization of these linkages in any of the compounds studied. It is worth noting that the pyridinium-substituted "arms" of the complexes will adopt various conformations due to rotations about the C−C single bonds. The spectroscopic and other measurements clearly probe the averaged properties of all possible structures that exist in solutions or frozen glasses. Because the C═C bonds are held in a fixed *E* configuration, the overall directionality of the ICT processes will not be greatly variable, but some parameters such as dipole moments may show some conformational dependency. However, given that all of the samples were studied under the same experimental conditions, comparisons between the data obtained are still expected to be valid.

For the purposes of Stark spectroscopy (see below), complex salts **2**, **8**, and **12** were converted into their tetraphenylborate analogues (denoted **2B**, **8B**, and **12B**) in order to give increased solubilities in the butyronitrile glassing medium. However, both the ^{1}H NMR spectra and CHN analyses show that anion metathesis is not complete, with as much as ca. 1.5 equiv of PF_6^- being retained in the products; this observation is unsurprising given the unusually large number of anions associated with each complex cation.

Electronic Spectroscopy Studies. The electronic absorption spectra of the new complex salts **2**, **4**−**6**, **8**, and **10**−**13** have been measured in acetonitrile, and the data are presented in Table 2. These spectra feature intense intraligand $\pi \rightarrow \pi^*$ absorptions in the UV region, together with intense, broad $d(M^{II}) \rightarrow \pi^*(L^A)$ (M = Ru/Fe, L^A = N-substituted bpy derivative) visible MLCT bands, with two maxima in each case. The energy separation between the two MLCT maxima lies in the range of 0.45−0.48 eV for the Ru^{II} complexes and 0.48−0.58 eV for their Fe^{II} analogues. The data for only the MLCT bands are collected in

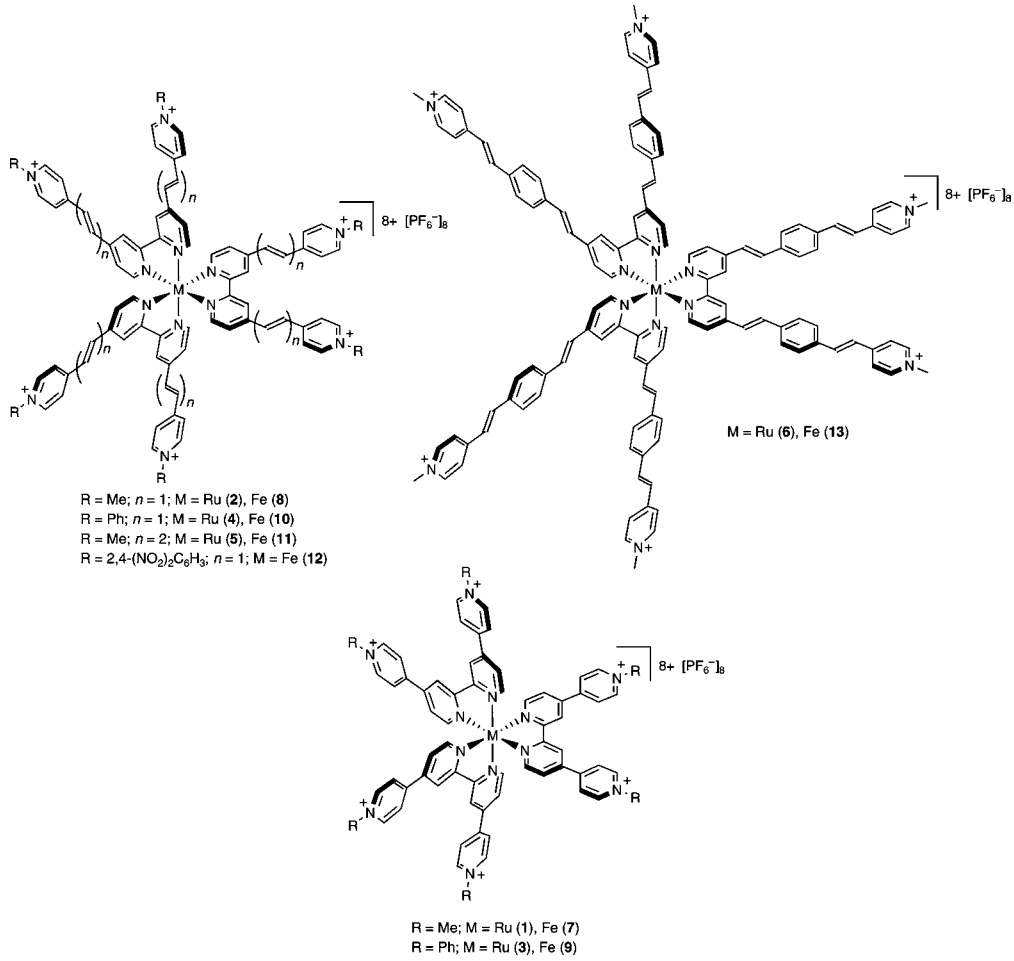

Figure 1. Chemical structures of the new complex salts investigated, together with the previously reported **1**, **3**, **7**, and **9**.[15]

Table 3, together with those for the previously reported related compounds **1**, **3**, **7**, and **9**[15] for comparison purposes. Representative UV−vis spectra of the complex salts **1**, **2**, **4**−**6**, **10**, and **13** are shown in Figures 2 and 3.

Considering the MLCT absorptions of the Ru^{II} complexes **1**, **2**, and **5** (Figure 2), the lower energy (LE) band shows a steady red shift as the conjugation within the ligands is extended, with sequential energy differences of 0.10 and 0.03 eV (Table 3). The energy of the higher energy (HE) band decreases by 0.25 eV on moving from **1** to **2** but then remains constant in **5**, although it should be noted that the error limits on the quoted HE maxima are large due to strong overlap with the LE band. The band intensities also increase steadily and substantially on moving along this series, due to the increasing extent of π-coupling. Comparison of the data for the *N*-Ph derivatives **3** and **4** reveals a similar pattern, with red shifts of 0.09 and 0.16 eV for the LE and HE bands, respectively. A concomitant ca. 2-fold enhancement in ϵ is also observed. The Me_2bbpvb^{2+}-containing complex in **6** shows only one discernible MLCT maximum (but with a high-energy shoulder; Figure 2) that lies to high energy of those of all the other new Ru^{II} chromophores, but to slightly lower energy in comparison with the qpy-based species **1** and **3**. A major difference between the latter and the new complexes is the increased intensities of the ILCT bands; for **1** and **3**, the lowest energy such absorptions are observed at 324 nm ($\epsilon = 55.0 \times 10^3$ M^{-1} cm^{-1}) and 328 nm ($\epsilon = 65.7 \times 10^3$ M^{-1} cm^{-1}), respectively.[15] As for the MLCT bands, this change is attributable to the presence of extended and more strongly coupled π-conjugated systems in **2** and **4**−**6**. The MLCT ϵ values quoted for **6** and **13** are strongly enhanced by overlap with the ILCT bands (Figures 2 and 3).

As noted previously for the qpy-based chromophores,[15] the MLCT bands of the Fe^{II} complexes are somewhat less intense and red-shifted in comparison with those of their Ru^{II} counterparts (Figure 3). On moving from **1** to **7**, the energy decrease for the LE band is ca. 0.39 eV and that for the HE band is ca. 0.33 eV. The corresponding changes for the pair **3** and **9** are 0.38 and 0.29 eV. For the new complexes, the shift of the LE absorption (−0.35 eV in all cases) on replacing Ru with Fe is slightly smaller than those for the analogous qpy-based chromophores. The shift for the HE band appears to vary over a range of ca. 0.25−0.30 eV, but this may not really be the case, due to the uncertainties in the E_{max} values. In contrast to the behavior of the MLCT absorptions, the intraligand bands are more intense in the Fe^{II} complexes in comparison with their Ru^{II} analogues. In keeping with our previous studies on various chromophores with *N*-arylpyridinium electron acceptor groups,[15,20,37] replacing a methyl with a phenyl substituent causes the MLCT bands to red-shift in every case; these decreases in energy for the HE bands are generally about twice those of the LE absorptions (Table 3). On moving from **10** to its $(2,4\text{-DNPh})_2bbpe^{2+}$ counterpart in **12**, further small red shifts are observed.

Taken in the context of the vast literature on transition-metal tris-chelate complexes of α-diimine ligands, our new chromophores, and especially the Me_2bbpvb^{2+}-containing species

Table 2. UV−Vis Absorption and Electrochemical Data for the New Complex Salts $[M^{II}(L^A)_3][PF_6]_8$ in Acetonitrile

				$E_{1/2}$, V vs Ag/AgCl (ΔE_p, mV)[b]	
salt (M/L^A)	λ_{max}, nm[a] (ϵ, 10^3 M^{-1} cm^{-1})	E_{max}, eV	assignment	$M^{III/II}$	L^A reduction
2 (Ru/Me_2bbpe^{2+})	506 (58.9)	2.45	d → π*	1.43 (90)	−0.67 (190)
	428 (40.5)	2.90	d → π*		−0.99[c]
	314 (159.4)	3.95	π → π*		
4 (Ru/Ph_2bbpe^{2+})	514 (75.6)	2.41	d → π*	1.42 (80)	−0.52[c]
	434 (49.2)	2.86	d → π*		−0.94 (130)
	329 (206.5)	3.77	π → π*		
5 (Ru/Me_2bbpb^{2+})	513 (80.1)	2.42	d → π*	1.32 (80)	−0.67[c]
	428 (61.6)	2.90	d → π*		−1.13[c]
	351 (215.4)	3.53	π → π*		
	255 (61.1)	4.86	π → π*		
6 (Ru/Me_2bbpvb^{2+})	501 (106.1)	2.48	d → π*	1.23 (90)	−0.83[c]
	385 (275.0)	3.22	π → π*		−0.99[c]
	307 (61.5)	4.04	π → π*		−1.78[c]
	247 (88.2)	5.02	π → π*		
8 (Fe/Me_2bbpe^{2+})	591 (40.9)	2.10	d → π*	1.19 (80)	−0.67 (180)
	468 (26.9)	2.65	d → π*		−1.10[c]
	317 (190.0)	3.91	π → π*		
	221 (60.2)	2.21	π → π*		
10 (Fe/Ph_2bbpe^{2+})	601 (50.7)	2.06	d → π*	1.19 (90)	−0.54[c]
	485 (31.7)	2.56	d → π*		−0.96 (120)
	336 (241.9)	3.69	π → π*		
11 (Fe/Me_2bbpb^{2+})	600 (56.6)	2.07	d → π*	1.08 (90)	−0.71[c]
	475 (38.5)	2.61	d → π*		−1.18[c]
	358 (274.7)	3.46	π → π*		
	251 (61.9)	4.94	π → π*		
12 ($Fe/(2,4\text{-}DNPh)_2bbpe^{2+}$)	611 (50.0)	2.03	d → π*	1.21 (100)	−0.30[c]
	495 (29.2)	2.51	d → π*		−0.98[c]
	333 (228.1)	3.72	π → π*		−1.31[c]
	226 (159.0)	5.49	π → π*		−1.39[c]
					−1.53[c]
13 (Fe/Me_2bbpvb^{2+})	581 (61.5)	2.13	d → π*	0.97 (80)	−0.87[c]
	458 (67.9)	2.71	d → π*		−1.05[c]
	385 (349.8)	3.22	π → π*		−1.84[c]
	246 (93.8)	5.04	π → π*		

[a] Solutions ca. $3-8 \times 10^{-5}$ M. [b] Measured in solutions ca. 10^{-3} M in analyte and 0.1 M in $[N(C_4H_9\text{-}n)_4]PF_6$ at a 2 mm glassy-carbon-disk working electrode with a scan rate of 200 mV s^{-1}. Ferrocene was used as the internal reference: $E_{1/2}$ = 0.43 V, ΔE_p = 80−90 mV. [c] E_{pc} for an irreversible reduction process.

6 and **13**, display unusually intense ICT absorptions. The underivatized complexes $[M^{II}(bpy)_3]^{2+}$ give MLCT ϵ values of ca. 1.3×10^4 M^{-1} cm^{-1} for M = Ru (λ_{max} 452 nm in acetonitrile)[38] and ca. 0.9×10^4 M^{-1} cm^{-1} for M = Fe (λ_{max} 522 nm in water).[39] In comparison with the latter, the LE MLCT band of **13** is approximately 7 times more intense (Table 2). Comparisons with more closely related species substituted with extended π-conjugated systems are of more immediate interest. Le Bozec and colleagues have reported a number of such species, and the most intense absorption band apparently reported is for a Zn^{II} complex of an azobenzene-derivatized bpy ligand.[11e] Thus, replacing the outer vinyl units in Me_2bbpvb^{2+} with N═N and swapping the *N*-methylpyridinium groups for $-N(^nBu)_2$ gives an ϵ value of 2.46×10^5 M^{-1} cm^{-1} for the ILCT band (λ_{max} 496 nm in dichloromethane); this intensity is slightly smaller than that observed for **6** but only about 70% of that for **13**. Indeed, to our knowledge the ILCT band for **13** is the most intense single absorption feature yet reported for a mononuclear complex of this type.

Electrochemical Studies. The new complex salts **2**, **4**−**6**, **8**, and **10**−**13** have been studied by cyclic voltammetry in acetonitrile, and the results are presented in Table 2. Selected data are also collected together with those for the previously reported qpy-based species **1**, **3**, **7**, and **9**[15] in Table 3. In general, these compounds give better defined electrochemistry when using a glassy-carbon working electrode rather than a platinum disk;[15] therefore, only data obtained by using the former are quoted here. Representative cyclic voltammograms of the complex salts **4** and **10** are shown in Figure 4.

All of the complexes show reversible or quasi-reversible $M^{III/II}$ (M = Ru, Fe) oxidation waves, together with reversible, quasi-reversible, and/or irreversible ligand-based reductions. The most obvious trend evident in these data is that the $E_{1/2}(Fe^{III/II})$ values are lower than the corresponding potentials for their Ru analogues by 210−260 mV (Figure 4), a consequence of the higher electron density at the Fe^{II} centers (Table 3).[15] This difference is also reflected in the red shifts observed for the MLCT bands (see above). For a given conjugated system in L^A, the $E_{1/2}(M^{III/II})$ values are not significantly affected by the nature of the N substituent, as observed for example in the series **8**, **10**, and **12**. However, extending the conjugation within the ligands does affect the potentials. For the series **1**, **2**, **5**, and **6**, $E_{1/2}(Ru^{III/II})$ decreases by respective increments of 170, 110, and 90 mV, while for the series **7**, **8**, **11**, and **13** the sequential changes in $E_{1/2}(Fe^{III/II})$ are 200, 110, and 110 mV. This trend is attributable to the cumulative electron-donating influence of the ethylene substituents, and it is apparent that the (*E*,*E*)-1,4-bis(vinyl)phenylene unit is more strongly donating than the (*E*,*E*)-1,3-butadienyl fragment. By way of comparison, inserting an (*E*)-vinyl unit into the *N*-methyl-4,4′-bipyridinium ligand in

(38) Juris, A.; Balzani, V.; Belser, P.; von Zelewsky, A. *Helv. Chim. Acta* **1981**, *64*, 2175–2182.
(39) Ford-Smith, M. H.; Sutin, N. *J. Am. Chem. Soc.* **1961**, *83*, 1830–1834.

Table 3. MLCT Absorption and Selected Electrochemical Data for Complex Salts **1**−**13** in Acetonitrile

			$E_{1/2}$ or E, V vs Ag/AgCl[b]	
salt (M/L^A)	λ_{max}, nm[a] (ϵ, 10^3 M^{-1} cm^{-1})	E_{max}, eV	$M^{III/II}$	L^A reduction
1 (Ru/Me_2qpy^{2+})[c]	486 (37.3)	2.55	1.60	−0.70
	394 (26.4)	3.15		
2 (Ru/Me_2bbpe^{2+})	506 (58.9)	2.45	1.43	−0.67
	428 (40.5)	2.90		
3 (Ru/Ph_2qpy^{2+})[c]	496 (37.3)	2.50	1.61	−0.53
	410 (26.1)	3.02		
4 (Ru/Ph_2bbpe^{2+})	514 (75.6)	2.41	1.42	−0.52[d]
	434 (49.2)	2.86		
5 (Ru/Me_2bbpb^{2+})	513 (80.1)	2.42	1.32	−0.67[d]
	428 (61.6)	2.90		
6 (Ru/Me_2bbpvb^{2+})	501 (106.1)	2.48	1.23	−0.83[d]
7 (Fe/Me_2qpy^{2+})[c]	574 (26.0)	2.16	1.39	−0.72[d]
	440 (18.8)	2.82		
8 (Fe/Me_2bbpe^{2+})	591 (40.9)	2.10	1.19	−0.67
	468 (26.9)	2.65		
9 (Fe/Ph_2qpy^{2+})[c]	584 (32.5)	2.12	1.39	−0.51[d]
	454 (22.0)	2.73		
10 (Fe/Ph_2bbpe^{2+})	601 (50.7)	2.06	1.19	−0.54[d]
	485 (31.7)	2.56		
11 (Fe/Me_2bbpb^{2+})	600 (56.6)	2.07	1.08	−0.71[d]
	475 (38.5)	2.61		
12 ($Fe/(2,4\text{-}DNPh)_2bbpe^{2+}$)	611 (50.0)	2.03	1.21	−0.30[d]
	495 (29.2)	2.51		
13 (Fe/Me_2bbpvb^{2+})	581 (61.5)	2.13	0.97	−0.87[d]
	458 (67.9)	2.71		

[a] Solutions ca. $3-8 \times 10^{-5}$ M. [b] Measured in solutions ca. 10^{-3} M in analyte and 0.1 M in $[N(C_4H_9\text{-}n)_4]PF_6$ at a 2 mm glassy-carbon-disk working electrode with a scan rate of 200 mV s^{-1}. Ferrocene was used as the internal reference: $E_{1/2} = 0.43$ V. [c] Data taken from ref 15. [d] E_{pc} for an irreversible reduction process.

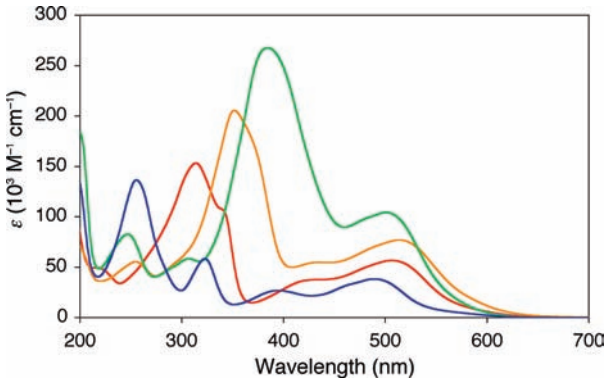

Figure 2. Electronic absorption spectra of **1** (blue), **2** (red), **5** (gold), and **6** (green) at 293 K in acetonitrile.

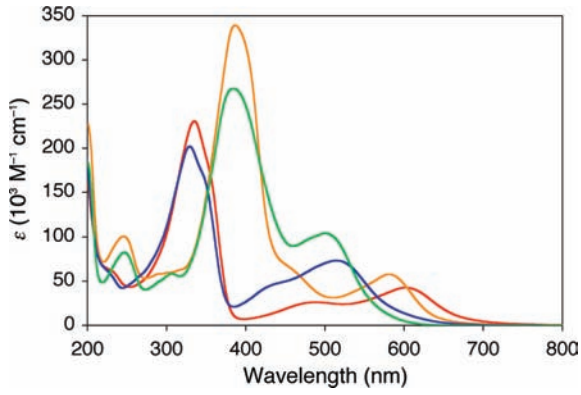

Figure 3. Electronic absorption spectra of **4** (blue), **6** (green), **10** (red), and **13** (gold) at 293 K in acetonitrile.

1D dipolar complexes causes $E_{1/2}(M^{III/II})$ to decrease by ca. 30−50 mV, while moving to a (*E*,*E*)-1,3-butadienyl or a (*E*,*E*)-1,4-bis(vinyl)phenylene bridge gives smaller additional changes of 0−30 mV.[21,40] These decreases in the $E_{1/2}(M^{III/II})$ values correlate with the steady red shifts observed in the LE MLCT bands (see above), except for the Me_2bbpvb^{2+} compounds.

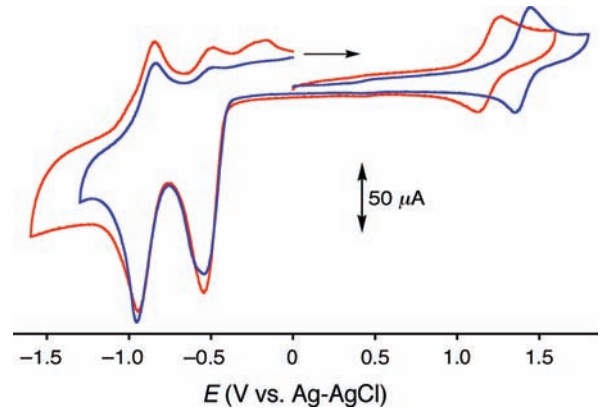

Figure 4. Cyclic voltammograms of **4** (blue) and **10** (red) in acetonitrile at 200 mV s^{-1} at a glassy-carbon working electrode (the arrow indicates the direction of the initial scans).

The often irreversible nature of the ligand-based reduction processes precludes further extensive discussion. However, it is apparent that the nature of the metal center does not significantly affect the potentials. Also, the first reduction wave is markedly sensitive to the N substituent, with all of the *N*-phenyl complexes showing higher potentials in comparison with their *N*-methyl analogues. A total anodic shift of 370 mV is observed moving along the series **8**, **10**, and **12**. This trend reflects the increasing electron-accepting ability of the pyri-

(40) Coe, B. J.; Foxon, S. P.; Harper, E. C.; Raftery, J.; Shaw, R.; Swanson, C. A.; Asselberghs, I.; Clays, K.; Brunschwig, B. S.; Fitch, A. G. *Inorg. Chem.* **2009**, *48*, 1370–1379.

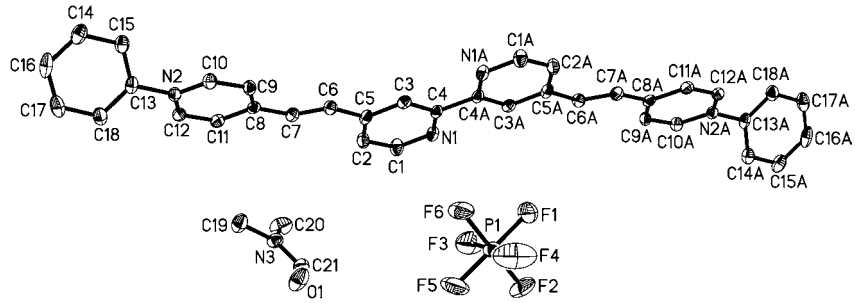

Figure 5. Representation of the molecular structure of the salt $[Ph_2bbpe^{2+}][PF_6]_2 \cdot 2DMF$, with H atoms omitted for clarity (50% probability ellipsoids). While the Ph_2bbpe^{2+} cation has been completed by generating symmetry-equivalent atoms, only the single PF_6^- anion and DMF molecule present in the asymmetric unit are shown.

Table 4. Selected Interatomic Distances (Å) and Angles (deg) for the Salt $[Ph_2bbpe^{2+}][PF_6]_2 \cdot 2DMF$

N(1)−C(4)	1.336(3)	C(8)−C(9)	1.392(3)
N(1)−C(1)	1.333(3)	C(8)−C(11)	1.394(3)
C(3)−C(4)	1.380(3)	C(9)−C(10)	1.356(3)
C(1)−C(2)	1.373(3)	C(11)−C(12)	1.349(3)
C(3)−C(5)	1.391(3)	N(2)−C(10)	1.358(3)
C(2)−C(5)	1.385(3)	N(2)−C(12)	1.354(3)
C(5)−C(6)	1.454(3)	N(2)−C(13)	1.436(3)
C(6)−C(7)	1.325(3)	C(4)−C(4)A	1.485(4)
C(7)−C(8)	1.449(3)		
C(5)−C(6)−C(7)	123.1(2)	C(6)−C(7)−C(8)	127.4(2)

dinium groups, as also manifested in the MLCT data (see above) and in previously reported related compounds.[15,20,37] The relatively large currents for the cathodic peaks in comparison with those for the metal-based waves (Figure 4) are consistent with multielectron processes attributable to simultaneous reductions of all three L^A ligands.

Crystallographic Study. Although we have unfortunately been unable to grow diffraction-quality crystals of any of the new complex salts, a single-crystal X-ray structure has been obtained for the proligand salt $[Ph_2bbpe^{2+}][PF_6]_2 \cdot 2DMF$. A representation of the molecular structure is shown in Figure 5, and selected interatomic distances and angles are presented in Table 4. We have also determined structures of the related compounds $[Ph_2qpy^{2+}][PF_6]_2 \cdot Me_2CO$[37] and $[Phbpe^+]Cl \cdot HCl \cdot H_2O$.[41]

As expected on the basis of steric considerations, the Ph_2bbpe^{2+} cation adopts a transoid configuration with a crystallographic center of symmetry in the middle of the C−C bond between the rings of the bpy group. The same applies to the related cation in $[Ph_2qpy^{2+}][PF_6]_2 \cdot Me_2CO$.[37] The π-conjugated bbpe unit in $[Ph_2bbpe^{2+}][PF_6]_2 \cdot 2DMF$ is close to planar, with a dihedral angle of 7.9° between the two pyridyl rings; this compares with a corresponding angle of 15.7° in $[Phbpe^+]Cl \cdot HCl \cdot H_2O$.[41] The dihedral angle between the quaternized pyridyl and attached phenyl rings in the latter is 53.4°,[41] somewhat larger than that observed in $[Ph_2bbpe^{2+}][PF_6]_2 \cdot 2DMF$ (44.5°). Such twists are attributable in part to steric interactions between the ortho hydrogen atoms of the two rings. All of the other geometric parameters are closely similar for both $[Ph_2bbpe^{2+}][PF_6]_2 \cdot 2DMF$ and $[Phbpe^+]Cl \cdot HCl \cdot H_2O$.[41]

Hyper-Rayleigh Scattering and Luminescence Studies. The β values of the complex salts **2**, **4**−**6**, **8**, and **10**−**13** were measured in acetonitrile solutions by using the HRS technique[28,29,31] with a 800 nm Ti^{3+}:sapphire laser, and the results are collected in Table 5, together with the previously published data for **1**, **3**, **7**, and **9**.[15] This wavelength was chosen originally because the latter complexes do not absorb strongly at either 800 nm or at the second harmonic (SH) of 400 nm, their MLCT bands falling conveniently between these wavelengths. However, several of the new, extended chromophores do show intense ILCT bands near 400 nm (Table 2, Figures 2 and 3), and the results obtained for these salts are hence strongly affected by resonance enhancement. In order to obtain additional data, we have therefore also used a 1064 nm Nd^{3+}:YAG laser to study these compounds, and the results are included in Table 5. A benefit of using a 800 or 1064 nm laser is the avoidance of any contributions due to two-photon luminescence. All of the Ru^{II} complexes emit at wavelengths above 670 nm (Table 5), with negligible emission below about 600 nm. In contrast, the Fe^{II} complexes are predictably nonemissive at room temperature. Within the series **1**, **2**, and **5**, the λ_{em} values red-shift steadily, consistent with the trend in the MLCT absorption maxima. However, the emission intensity is significantly weaker for **5** in comparison with those for **1** and **2**. Comparison of the λ_{em} data for **3** and **4** also reveals a red shift, while the emission band for **6** falls between those of **2** and **4**. The experimentally determined β values for each operating wavelength are based on the assumption of a single tensor component, β_{xxx}, and are derived from the total HRS intensity $\langle\beta_{HRS}^2\rangle$ by using the equation

$$\langle\beta_{HRS}^2\rangle = \left(\frac{8}{35} + \frac{16}{105}\right)\beta_{xxx}^2 = \left(\frac{8}{21}\right)\beta_{xxx}^2 \qquad (7)$$

While the effects of resonance preclude a detailed analysis of the HRS results, some trends are apparent. First, extending the ligand conjugated systems leads to steadily increasing β values in all instances except for the *N*-phenylated pair **3** and **4** when studied at 800 nm (Table 5). It is well established that β responses normally increase as conjugated systems are extended,[1] although the very large values obtained for **2** and **4**−**6** can be attributed in large part to resonance enhancement. The second trend that emerges from the collected data is that the Ru-based chromophores give larger β values than their Fe analogues in all cases except for the Me_2bbpe^{2+}-containing pair **2** and **8** when studied at 800 nm. However, the $\beta_{xxx,1064}$ value for **2** is about 3 times that for **8**. Comparison within the Fe-based series **8**, **10**, and **12** does not reveal the steady increases in $\beta_{xxx,800}$ that might be expected on the basis of the decreasing

(41) Coe, B. J.; Foxon, S. P.; Harper, E. C.; Helliwell, M.; Raftery, J.; Swanson, C. A.; Brunschwig, B. S.; Clays, K.; Franz, E.; Garín, J.; Orduna, J.; Horton, P. N.; Hursthouse, M. B. *J. Am. Chem. Soc.* **2010**, *132*, 1706–1723.

Table 5. MLCT Absorption, Luminescence, and HRS Data for Complex Salts **1**−**13** in Acetonitrile

salt (M/L^A)	λ_{max}, nm	λ_{em}, nm[a]	$\beta_{xxx,800}$,[b] 10^{-30} esu	$\beta_{xxx,1064}$,[c] 10^{-30} esu
1 (Ru/Me_2qpy^{2+})[d]	486, 394	671	170 ± 21	*e*
2 (Ru/Me_2bbpe^{2+})	506, 428	712	190 ± 35	850 ± 160
3 (Ru/Ph_2qpy^{2+})[d]	496, 410	685	270 ± 35	*e*
4 (Ru/Ph_2bbpe^{2+})	514, 434	724	170 ± 30	1200 ± 600
5 (Ru/Me_2bbpb^{2+})	513, 428	764[f]	1200 ± 400	3100 ± 700
6 (Ru/Me_2bbpvb^{2+})	501	718	1500 ± 300	5600 ± 1300
7 (Fe/Me_2qpy^{2+})[d]	574, 440	*g*	78 ± 10	*e*
8 (Fe/Me_2bbpe^{2+})	591, 468	*g*	320 ± 110	275 ± 110
9 (Fe/Ph_2qpy^{2+})[d]	584, 454	*g*	80 ± 10	*e*
10 (Fe/Ph_2bbpe^{2+})	601, 485	*g*	90 ± 30	480 ± 80
11 (Fe/Me_2bbpb^{2+})	600, 475	*g*	340 ± 180	340 ± 200
12 (Fe/(2,4-DNPh)$_2$bbpe^{2+})	611, 495	*g*	145 ± 40	400 ± 140
13 (Fe/Me_2bbpvb^{2+})	581, 458	*g*	660 ± 130	700 ± 200

[a] Emission maximum upon excitation into the MLCT bands (λ_{ex} 480 nm for **2** and **5**, 514 nm for **4**, and 510 nm for **6**), with ca. 10^{-5} M solutions; dilution produced no changes in the λ_{em} values. [b] First hyperpolarizability measured by using a 800 nm Ti^{3+}:sapphire laser. [c] First hyperpolarizability measured by using a 1064 nm Nd^{3+}:YAG laser. The quoted cgs units (esu) can be converted into SI units (C^3 m^3 J^{-2}) by dividing by a factor of 2.693×10^{20}. [d] Data taken from ref 15. [e] Not measured. [f] Relatively weak signal. [g] Not observed.

MLCT energies or previous studies with related 1D complexes.[42] In contrast, **8** does show the smallest $\beta_{xxx,1064}$ value of these three compounds.

Stark Spectroscopic Studies. Complex salts **2B**, **4**−**6**, **8B**, **10**, **11**, **12B**, and **13** have been studied by Stark spectroscopy[33] in butyronitrile glasses at 77 K, and the results are presented in Table 6, together with the previously published data for **1**, **3**, **7**, and **9**.[15] Gaussian fitting of the MLCT absorption spectra using three or four curves was necessary to successfully model the Stark data. It is likely that the ILCT transitions in the extended chromophores, especially **5**, **6**, **11**, and **13**, will contribute substantially to their NLO responses. However, these bands could be analyzed only for **6** and **13** because the short-wavelength operational cutoff of our Stark spectrometer is about 350 nm. For both **6** and **13**, the entire ICT region was treated as one. In the case of **6**, strong overlap between the MLCT and ILCT bands means that it is not possible to fully resolve the two types of transition and a total of eight curves was used. In contrast, for **13** there is a relatively good degree of separation between the MLCT and ILCT bands; three curves were then used for the former and four for the latter, with some overlap even so. The resulting data for **6** and **13** are included in Table 6. Representative absorption spectra and electroabsorption spectra in the MLCT region for the complex salts **2B**, **5**, and **8B** are shown in Figure 6, while the full ICT region spectra for for **6** and **13** are shown in Figure 7. The MLCT region spectra for all of the other new complex salts are provided as Supporting Information (Figures S1 and S2).

As noted previously for **1** and **3**, for each of the Ru complexes a relatively low intensity Gaussian curve was placed to low energy in order to fit the Stark signal satisfactorily; these curves may correspond with spin-forbidden transitions to triplet MLCT excited states.[43] For **1**, **3**, **7**, and **9**, only two of the three Gaussian curves used to fit the transitions to singlet excited states contribute significantly to the observed Stark signals; therefore, the data obtained for the other functions are not quoted. However, for all of the new complex salts the latter are significant contributors; thus, the corresponding data are included in Table 6.

For the MLCT bands, the E_{max} values for the two most intense Gaussian curves fitted to the absorption spectra at 77 K in butyronitrile are generally decreased in comparison with the data recorded in acetonitrile solutions (Table 3). In almost every instance, the data obtained at 77 K show the same trends as those observed at room temperature: i.e., the red-shifting effects arising from extending the conjugated systems, replacing Ru with Fe, or replacing *N*-methyl with *N*-phenyl/2,4-dinitrophenyl substituents (see above). In order to analyze the f_{os} and μ_{12} data, it is appropriate to consider the totals for the various components, since the superposition of these gives the overall absorption profiles. The total f_{os} and μ_{12} values measured at 77 K show trends that generally correlate with those observed in the ϵ values in acetonitrile solutions (Table 3). Thus, the MLCT intensities increase when the conjugated systems are extended or when a *N*-methyl is replaced with a *N*-phenyl/2,4-dinitrophenyl substituent. Also, the Fe complexes show lower total f_{os} and μ_{12} values in comparison with their Ru analogues. This latter observation also applies to the combined MLCT and ILCT data for **6** and **13**.

The derived adiabatic and diabatic dipole moment changes ($\Delta\mu_{12}$ and $\Delta\mu_{ab}$, respectively) for the MLCT bands cover a broad range of ca. 5−34 D, with the largest being measured for one of the Gaussian components for **13**. For the purpose of analyzing and comparing these parameters, it is reasonable to consider average values because the fitted Gaussian components represent hypothetical ICT transitions that are codirectional but not additive in terms of their dipole moment changes. Both $\Delta\mu_{12}$ and $\Delta\mu_{ab}$ generally increase in a logical fashion as the conjugated systems are extended: for example, on moving along the Ru series **1** → **2B** → **5**. Except for the pair **1** and **3**, a pattern of increasing $\Delta\mu_{12}$ and $\Delta\mu_{ab}$ on replacing *N*-methyl with *N*-phenyl substituents is also observed, and steady increases occur on moving along the Fe series **8B** → **10** → **12B**. Overall, there is no clear trend in the dipole moment changes on varying the metal center. Since they derive directly from these data, the average delocalized and localized electron-transfer distances (r_{12} and r_{ab}, respectively) show the same trends, with r_{ab} exceeding 5 Å in several instances and being as high as 7 Å for **13**. Although the parameters c_b^2 and H_{ab} might be expected to decrease steadily with extension of the conjugated systems, the data obtained do not provide convincing evidence for such behavior, especially since the estimated errors on the c_b^2 values are very large.

(42) (a) Coe, B. J.; Harris, J. A.; Harrington, L. J.; Jeffery, J. C.; Rees, L. H.; Houbrechts, S.; Persoons, A. *Inorg. Chem.* **1998**, *37*, 3391–3399. (b) Coe, B. J.; Harries, J. L.; Harris, J. A.; Brunschwig, B. S.; Coles, S. J.; Light, M. E.; Hursthouse, M. B. *Dalton Trans.* **2004**, 2935–2942.

(43) Kober, E. M.; Meyer, T. J. *Inorg. Chem.* **1982**, *21*, 3967–3977.

Table 6. ICT Absorption and Stark Spectroscopic Data for Complex Salts **1**−**13**

salt (M/L^A)	ν_{max},[a] cm^{-1}	λ_{max},[a] nm	E_{max},[a] eV	f_{os}	μ_{12},[b] D	$\Delta\mu_{12}$,[c] D	$\Delta\mu_{ab}$,[d] D	r_{12},[e] Å	r_{ab},[f] Å	c_b^{2} [g]	H_{ab},[h] 10^3 cm^{-1}	β_0,[i] 10^{-30} esu	$\Sigma\beta_0$, 10^{-30} esu	N [j]	β_{EN},[k] 10^{-32} esu
1 (Ru/Me$_2$qpy^{2+})[l]	17 359	576	2.15	0.002	0.5	12.9	12.9	2.7	2.7	0.00	0.7	1	68	72	11.1
	20 149	496	2.50	0.17	4.2	7.9	11.6	1.6	2.4	0.16	7.4	26			
	25 240	396	3.13	0.39	5.8	10.3	15.5	2.2	3.2	0.17	9.4	41			
2B (Ru/Me$_2$bbpe^{2+})	17 421	574	2.16	0.07	2.9	17.4	18.4	3.6	3.8	0.02	2.8	37	191	84	24.8
	19 115	523	2.37	0.32	6.0	13.0	17.7	2.7	3.7	0.13	6.5	98			
	21 132	473	2.62	0.19	4.3	9.6	13.0	2.0	2.7	0.13	7.1	30			
	23 309	429	2.89	0.16	3.8	12.9	14.9	2.7	3.1	0.07	5.9	26			
3 (Ru/Ph$_2$qpy^{2+})[l]	16 998	589	2.11	0.02	1.4	7.0	7.5	1.5	1.6	0.04	3.2	4	114	108	10.2
	19 901	502	2.47	0.16	4.2	10.0	13.1	2.1	2.7	0.12	6.4	34			
	24 553	407	3.04	0.51	6.7	13.5	19.0	2.8	4.0	0.14	8.6	76			
4 (Ru/Ph$_2$bbpe^{2+})	17 664	566	2.19	0.27	5.7	22.8	25.4	4.8	5.3	0.05	4.0	181	586	120	44.6
	18 712	534	2.32	0.39	6.7	15.9	20.7	3.3	4.3	0.12	6.0	146			
	20 164	496	2.50	0.32	5.8	15.7	19.5	3.3	4.1	0.10	6.0	101			
	22 100	452	2.74	0.52	7.1	21.2	25.5	4.4	5.3	0.08	6.1	158			
5 (Ru/Me$_2$bbpb^{2+})	17 180	582	2.13	0.12	3.7	20.6	21.9	4.3	4.6	0.03	2.8	73	451	96	47.9
	18 712	534	2.32	0.56	8.0	15.8	22.4	3.3	4.7	0.14	6.6	217			
	20 486	488	2.54	0.40	6.5	14.7	19.6	3.1	4.1	0.12	6.5	111			
	22 422	446	2.78	0.21	4.5	16.6	18.8	3.5	3.9	0.06	5.3	50			
6 (Ru/Me$_2$bbpvb^{2+})	17 451	573	2.16	0.12	3.8	22.9	24.1	4.8	5.0	0.02	2.7	81	1078	132	71.1
	19 144	522	2.37	1.10	11.1	15.4	27.0	3.2	5.6	0.21	7.9	393			
	20 978	477	2.60	0.49	7.1	16.4	21.7	3.4	4.5	0.12	6.8	141			
	22 896	437	2.84	1.28	10.9	18.1	28.4	3.8	5.9	0.18	8.8	313			
	24 396	410	3.02	1.00	9.4	4.7	19.4	1.0	4.0	0.38	11.8	53			
	25 326	395	3.14	0.68	7.6	6.0	16.3	1.3	3.4	0.31	11.8	41			
	26 239	381	3.25	1.21	9.9	5.1	20.5	1.1	4.3	0.37	12.7	56			
	27 602	362	3.42	0.57	6.6	0.0	13.3	0.0	2.8	0.50	13.8	0			
7 (Fe/Me$_2$qpy^{2+})[l]	17 225	581	2.14	0.16	4.4	6.1	10.6	1.3	2.2	0.22	7.1	30	86	72	14.1
	22 531	444	2.79	0.35	5.8	11.2	16.1	2.3	3.4	0.15	8.1	56			
8B (Fe/Me$_2$bbpe^{2+})	16 292	614	2.02	0.11	3.9	10.1	12.7	2.1	2.7	0.10	4.9	44	197	84	25.6
	16 534	605	2.05	0.26	5.8	9.7	15.1	2.0	3.2	0.08	6.4	91			
	20 486	488	2.54	0.18	4.3	18.5	20.4	3.9	4.3	0.05	4.4	62			
9 (Fe/Ph$_2$qpy^{2+})[l]	16 950	590	2.10	0.16	4.5	7.4	11.6	1.5	2.4	0.18	6.5	39	121	108	10.8
	21 675	461	2.69	0.37	6.1	13.9	18.4	2.9	3.8	0.12	7.1	82			
10 (Fe/Ph$_2$bbpe^{2+})	16 050	623	1.99	0.19	5.1	11.6	15.4	2.4	3.2	0.12	5.2	87	477	120	36.3
	16 534	605	2.05	0.43	7.4	13.2	19.8	2.8	4.1	0.17	6.2	201			
	19 680	508	2.44	0.41	6.7	21.9	25.6	4.5	5.3	0.07	5.1	189			
11 (Fe/Me$_2$bbpb^{2+})	16 131	620	2.00	0.21	5.3	11.2	15.4	2.3	2.4	0.13	5.5	90	480	96	51.0
	16 696	599	2.07	0.45	7.6	11.0	18.8	2.3	3.9	0.20	6.8	173			
	19 922	502	2.47	0.47	7.1	22.5	26.6	4.7	5.5	0.08	5.3	217			
12B (Fe/(2,4-DNPh)$_2$bbpe^{2+})	15 808	633	1.96	0.11	3.8	12.6	14.8	2.6	3.1	0.07	4.1	56	416	132	27.4
	16 292	614	2.02	0.28	6.1	16.8	20.8	3.5	4.3	0.10	4.8	180			
	19 438	514	2.41	0.29	5.7	27.6	29.9	5.8	6.2	0.04	3.7	180			
13 (Fe/Me$_2$bbpvb^{2+})	16 569	604	2.05	0.42	7.4	10.0	17.8	2.1	3.7	0.22	6.9	150	836 (450)[m]	132	55.1 (29.7)[m]
	17 833	561	2.21	0.16	4.4	8.8	12.5	1.8	2.6	0.15	6.3	41			
	20 675	484	2.56	0.46	6.9	30.7	33.7	6.4	7.0	0.04	4.2	259			
	23 818	420	2.95	0.86	8.8	5.8	18.5	1.2	3.9	0.34	11.3	60			
	24 635	406	3.05	1.44	11.2	10.9	24.9	2.3	5.2	0.28	11.1	170			
	25 561	391	3.17	1.18	9.9	8.9	21.7	1.8	4.5	0.30	11.7	101			
	26 759	374	3.32	0.97	8.8	6.7	18.8	1.4	3.9	0.32	12.5	55			

[a] Maxima for Gaussian functions used to fit to spectral data recorded in butyronitrile glass at 77 K. [b] Calculated using eq 2; f_{os} obtained from $(4.60 \times 10^{-9}$ M cm$^2)\epsilon_{max} \times fw_{1/2}$, where ϵ_{max} is the maximal molar extinction coefficient and $fw_{1/2}$ is the full width at half height (in wavenumbers). [c] Calculated from $f_{int}\Delta\mu_{12}$ using $f_{int} = 1.33$. [d] Calculated from eq 1. [e] Delocalized electron-transfer distance calculated from $\Delta\mu_{12}/e$. [f] Effective (localized) electron-transfer distance calculated from $\Delta\mu_{ab}/e$. [g] Calculated from eq 3. [h] Calculated from eq 4. [i] Calculated from eq 5. [j] The total number of π-bonding electrons (excluding metal d-electrons) in the complex cation. [k] Electron-normalized off-resonant first hyperpolarizability, defined as $\Sigma\beta_0/N^{3/2}$.[50] [l] Data taken from ref 15. [m] The total contribution associated with (largely) only the MLCT transitions is in brackets for purposes of comparison with the other compounds.

As in our previous studies,[15] we have used the standard two-state model (eq 5)[44] to estimate static first hyperpolarizabilities from the Stark data for the transitions to dipolar ICT excited states. Although metal tris-chelate complexes have octupolar ground-state structures,[7] their NLO responses are clearly associated largely with dipolar ICT transitions. In this context, it is also important to note that other two-state descriptions are also available, which would alter the Stark-derived β_0 values quoted here by a constant factor of 0.5 or 2.[45] These data may hence be used primarily as a means to reveal structure−activity relationships involving all contributing ICT transitions without any interference from variable resonance effects, rather than necessarily revealing the absolute magnitudes of β_0. Even so, it is remarkable that our previous studies with dipolar Ru^{II} ammine complexes demonstrate that using the two-state equation (5) with a prefactor of 3 (the "perturbation series convention")[45]

(44) (a) Oudar, J. L.; Chemla, D. S. *J. Chem. Phys.* **1977**, *66*, 2664–2668. (b) Oudar, J. L. *J. Chem. Phys.* **1977**, *67*, 446–457.

(45) Willetts, A.; Rice, J. E.; Burland, D. M.; Shelton, D. P. *J. Chem. Phys.* **1992**, *97*, 7590–7599.

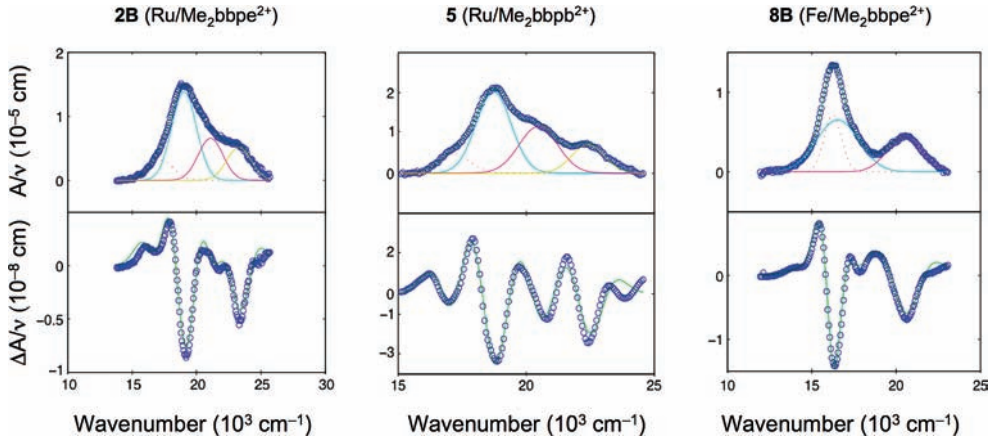

Figure 6. MLCT and Stark spectra with calculated fits for complex salts **2B**, **5**, and **8B** in an external electric field of 4.74×10^7 V m^{-1}: (top panels) absorption spectra illustrating Gaussian curves used in data fitting; (bottom panels) electroabsorption spectra, with experimental data shown in blue and fits in green according to the Liptay equation.[33]

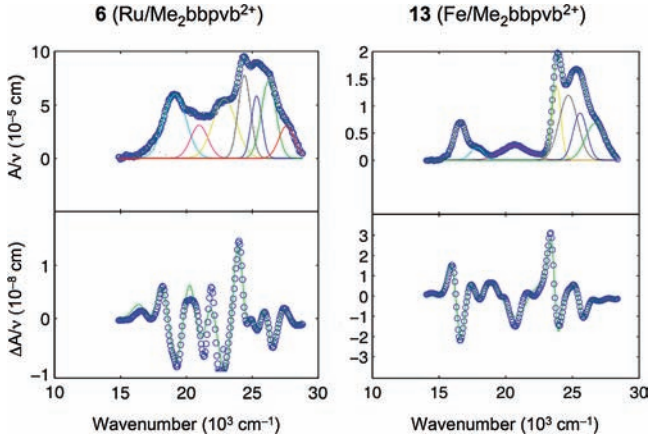

Figure 7. ICT and Stark spectra with calculated fits for complex salts **6** and **13** in an external electric field of 5.36×10^7 V m^{-1}: (top panels) absorption spectra illustrating Gaussian curves used in data fitting; (bottom panels) electroabsorption spectra, with experimental data shown in blue and fits in green according to the Liptay equation.[33]

often gives excellent quantitative agreement with the β_0 values determined via HRS with a 1064 nm laser.[32b]

We have shown in several previous studies that while using deconvolution is required to give satisfactory fits to the Stark data, the total $[\beta_0]_{ICT}$ values that arise from such treatment are generally very similar to those obtained without deconvolution.[41,46] These precedents confirm the reliability of this indirect approach to deriving β_0 responses. While it is probably of little value to consider the data for the individual Gaussian components in detail due to the uncertainties involved in the spectral deconvolution, the resulting total β_0 responses do merit further comments. First, sequential and dramatic increases are observed on extending the conjugated systems in moving along the Ru series **1** → **2B** → **5** or the Fe series **7** → **8B** → **11**, with the Me_2bbpb^{2+}-containing chromophores having estimated total MLCT-associated β_0 values about 6 times larger than those of their previously reported qpy-based counterparts. Moving from **11** to **13** does not change $\sum\beta_0$ significantly when considering only the MLCT-based contributions, but the total β_0 response derived for **13** is increased almost 2-fold when the ILCT contributions are included. Large increases in $\sum\beta_0$ also accompany the insertion of (*E*)-vinyl bridges into the *N*-phenyl chromophores, i.e. on moving from **3** to **4** and from **9** to **10**.

The second trend observed in the $\sum\beta_0$ values is that these increase substantially (ca. 1.5−3 times) on replacing *N*-methyl with more strongly electron-accepting *N*-phenyl substituents. Both of these trends evident in the $\sum\beta_0$ values for **1**−**13** reflect those we have observed previously when analyzing the MLCT bands for related 1D metallochromophores.[21,32b,40,42b] Although the *N*-2,4-dinitrophenyl substituent is an even more powerful electron acceptor according to the MLCT energies and ligand-based reduction potentials (see above), the total β_0 response derived for **12B** is possibly slightly smaller than that for **10**. This result can be attributed largely to the decreased MLCT transition intensities caused by diminished π-orbital overlap due to twisting of the 2,4-DNPh group with respect to the rest of the conjugated systems; this effect is especially evident in the f_{os} and μ_{12} values measured at 77 K (Table 6). It is, however, worth noting that our previous Stark studies have shown that replacing *N*-Ph with 2,4-DNPh substituents leads to increases in β_0, in both metal complexes[42b] and purely organic chromophores.[47] Also in contrast with the HRS results (see above), the estimated $\sum\beta_0$ values for **1**−**13** taken as a whole do not provide any clear indication that the nature of the metal center substantially affects the NLO responses. Although $\sum\beta_0$ appears to decrease considerably on replacing Ru with Fe in two instances (pairs **4**/**10** and **6**/**13**), the differences are within the experimental error limits.

It is not appropriate to attempt direct, quantitative comparisons between HRS and Stark-derived β values, because of the importance of resonance effects in HRS measurements and the potential uncertainty about the prefactor in eq 5 (see above). The challenges inherent in obtaining reliable β_0 data, especially from HRS studies, have been discussed previously.[48] Unfortunately, it is not possible to use this technique to derive anything

(46) Coe, B. J.; Foxon, S. P.; Harper, E. C.; Harris, J. A.; Helliwell, M.; Raftery, J.; Asselberghs, I.; Clays, K.; Franz, E.; Brunschwig, B. S.; Fitch, A. G. *Dyes Pigments* **2009**, *82*, 171–186.

(47) Coe, B. J.; Harris, J. A.; Asselberghs, I.; Wostyn, K.; Clays, K.; Persoons, A.; Brunschwig, B. S.; Coles, S. J.; Gelbrich, T.; Light, M. E.; Hursthouse, M. B.; Nakatani, K. *Adv. Funct. Mater.* **2003**, *13*, 347–357.

(48) Selected examples: (a) Woodford, J. N.; Wang, C. H.; Jen, A. K.-Y. *Chem. Phys.* **2001**, *271*, 137–143. (b) Di Bella, S. *New J. Chem.* **2002**, *26*, 495–497. (c) Tai, O. Y.-H.; Wang, C. H.; Ma, H.; Jen, A. K.-Y. *J. Chem. Phys.* **2004**, *121*, 6086–6092. (d) Campo, J.; Wenseleers, W.; Goovaerts, E.; Szablewski, M.; Cross, G. H. *J. Phys. Chem. C* **2008**, *112*, 287–296.

Table 7. Cubic NLO Parameters for Complex Salts **1**−**13** at 750 nm

salt (M/L^A)	γ_{real}, 10^{-36} esu	γ_{imag}, 10^{-36} esu	$\lvert\gamma\rvert$, 10^{-36} esu	σ_2, GM[a]
1 (Ru/Me_2qpy^{2+})[b]	−4300 ± 600	220 ± 30	4300 ± 600	62 ± 8
2 (Ru/Me_2bbpe^{2+})	−3000 ± 1500	2600 ± 300	4000 ± 1500	720 ± 90
3 (Ru/Ph_2qpy^{2+})[b]	−5800 ± 1500	420 ± 100	5800 ± 1500	120 ± 25
4 (Ru/Ph_2bbpe^{2+})	−9000 ± 1000	4200 ± 200	9900 ± 1000	1200 ± 50
5 (Ru/Me_2bbpb^{2+})	−12000 ± 2000	5200 ± 600	13100 ± 2000	1500 ± 170
6 (Ru/Me_2bbpvb^{2+})	−24000 ± 6000	8900 ± 900	25600 ± 6000	2500 ± 250
7 (Fe/Me_2qpy^{2+})[b]	−7400 ± 800	48 ± 15	7400 ± 800	13 ± 4
8 (Fe/Me_2bbpe^{2+})	−1700 ± 1000	1200 ± 150	2100 ± 1000	350 ± 40
9 (Fe/Ph_2qpy^{2+})[b]	−6400 ± 1500	13 ± 6	6400 ± 1500	3.6 ± 2
10 (Fe/Ph_2bbpe^{2+})	−11000 ± 2000	2200 ± 400	11200 ± 2000	600 ± 100
11 (Fe/Me_2bbpb^{2+})	−13000 ± 4000	5500 ± 700	14100 ± 4000	1500 ± 200
12 (Fe/(2,4-DNPh)$_2$bbpe^{2+})	−21000 ± 2000	950 ± 120	21000 ± 2000	265 ± 30
13 (Fe/Me_2bbpvb^{2+})	−18000 ± 3000	5100 ± 300	18700 ± 3000	1400 ± 100

[a] 1 GM = 10^{-50} cm^4 s photon^{-1}. [b] Data taken from ref 16.

more than resonance-enhanced β values for compounds that display more than one ICT band. Therefore, the Stark-derived β_0 data we report for **1**−**13** give the most accurate description of the (relative) NLO responses of this series of chromophores. However, it should also be emphasized that the β_0 values for most of the new complex chromophores are only lower limits, since they do not account for contributions associated with the ILCT transitions. In Ru^{II} ammine complexes of monodentate ligands related to Me_2bbpb^{2+}, the ILCT processes account for ca. 10−20% of the total estimated β_0 values.[21,41] Given that the tris-chelate derivatives contain six individual π-conjugated "arms", the total ILCT contributions to β_0 will be larger when compared with related 1D or 2D systems. Nevertheless, the MLCT-associated responses achieved of ca. (400−600) × 10^{-30} esu for **4**, **5**, **10**, and **11** are among the largest (off-resonance) quadratic NLO responses determined for metal-containing chromophores. Furthermore, the $\sum\beta_0$ values for **6** and **13** are possibly the highest yet recorded. These results serve to highlight the utility of the Stark-based approach, which is the only method by which such data for chromophores with relatively complicated ICT spectra may be obtained. In order to set these results in context, it is worth considering data obtained by applying the Stark-based approach to a benchmark chromophore, under the same experimental conditions and using eq 5. The salt (*E*)-4′-(dimethylamino)-*N*-methyl-4-stilbazolium (DAS) tosylate[49] is the first organic NLO material to become commercialized (for THz wave generation via nonlinear frequency mixing). We have derived previously a β_0 value of 236 × 10^{-30} esu for [DAS]PF_6,[47] substantially smaller than most of those determined for the new compounds (Table 6).

It is well established that hyperpolarizabilities generally increase with the size of the π-conjugated system.[1] In attempts to assess the extent to which quadratic NLO responses are also influenced by other factors and to probe their fundamental quantum limits, recent studies with purely organic dipolar chromophores have included electron-normalized off-resonant

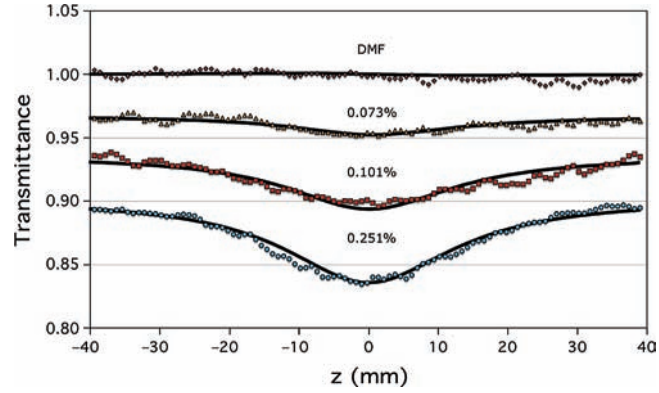

Figure 8. Examples of open-aperture Z-scans on **11** in DMF solutions at 750 nm. Full lines denote theoretically computed curves.

first hyperpolarizabilities β_{EN},[50] which are derived by considering the total number of π-bonding electrons. We have therefore calculated β_{EN} values for **1**−**13**, and these are included in Table 6. These data confirm substantial enhancements in the NLO response on moving along the series **1** → **2B** → **5** and **7** → **8B** → **11**. Replacing R = Me with R = Ph gives *lower* β_{EN} values for the qpy-based species but *higher* values for their bbpe-based counterparts. The series **8B** → **10** → **12B** shows an increase in β_{EN} on moving from R = Me to R = Ph, but then a decrease for the 2,4-DNPh-containing complex. The application of this approach to the Stark-derived β_0 values for stilbazolium and closely related organic chromophores[46,47] also indicates that the β_{EN} responses of *N*-Ph species are larger than those of their 2,4-DNPh analogues.[51]

Two-Photon Absorption Studies. The new complex salts **2**, **4**−**6**, **8**, and **10**−**13** were investigated in DMF solutions by using the Z-scan technique[34,35] at a laser wavelength of 750 nm, to afford the real and imaginary parts of γ together with the 2PA cross sections σ_2. The results are collected in Table 7, along with the data published previously for **1**, **3**, **7**, and **9**.[16] Figure 8 shows an example set of open-aperture Z-scans on **11** showing the concentration dependence of the dip due to 2PA. The curves are shifted due to the presence of some one-photon absorption in solutions of **11** at 750 nm.

All of the complex salts **1**−**13** show relatively strong negative refractive nonlinearity, as indicated by their γ_{real} values (Table

(49) Selected examples: (a) Kawase, K.; Mizuno, M.; Sohma, S.; Takahashi, H.; Taniuchi, T.; Urata, Y.; Wada, S.; Tashiro, H.; Ito, H. *Opt. Lett.* **1999**, *24*, 1065–1067. (b) Kawase, K.; Hatanaka, T.; Takahashi, H.; Nakamura, K.; Taniuchi, T.; Ito, H. *Opt. Lett.* **2000**, *25*, 1714–1716. (c) Taniuchi, T.; Okada, S.; Nakanishi, H. *Appl. Phys. Lett.* **2004**, *95*, 5984–5988. (d) Taniuchi, T.; Ikeda, S.; Okada, S.; Nakanishi, H. *Jpn. J. Appl. Phys.* **2005**, *44*, L652–L654. (e) Schneider, A.; Neis, M.; Stillhart, M.; Ruiz, B.; Khan, R. U. A.; Günter, P. *J. Opt. Soc. Am. B* **2006**, *23*, 1822–1835. (f) Schneider, A.; Stillhart, M.; Günter, P. *Opt. Express* **2006**, *14*, 5376–5384. (g) Yang, Z.; Mutter, L.; Stillhart, M.; Ruiz, B.; Aravazhi, S.; Jazbinsek, M.; Schneider, A.; Gramlich, V.; Günter, P. *Adv. Funct. Mater.* **2007**, *17*, 2018–2023.

(50) (a) Kuzyk, M. G. *Phys. Rev. Lett.* **2000**, *85*, 1218–1221. (b) Kuzyk, M. G. *Phys. Rev. Lett.* **2003**, *90*, 039902. (c) Tripathy, K.; Pérez Moreno, J.; Kuzyk, M. G.; Coe, B. J.; Clays, K.; Myers Kelley, A. *J. Chem. Phys.* **2004**, *121*, 7932–7945.

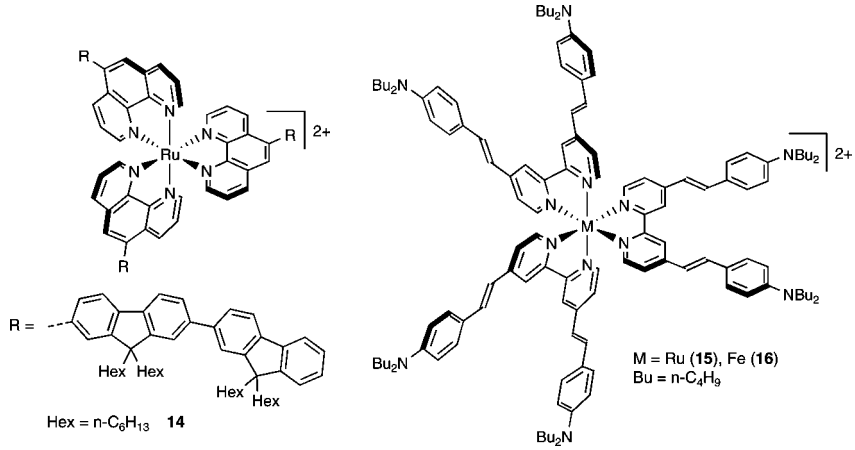

Figure 9. Chemical structures of some complex chromophores investigated for 2PA purposes previously.[12]

7). Such behavior is typical for molecules probed at wavelengths in the vicinity of strong one- or two-photon absorptions. Several trends are evident in the 2PA data. (i) Extending the conjugated systems of the ligands leads to large increases in activity, as expected on the basis of previous reports concerning purely organic chromophores. On moving along the Ru series **1** → **2** → **5**, a total σ_2 enhancement of ca. 24-fold is observed, while the corresponding increase for the Fe series **7** → **8** → **11** is ca. 115-fold. (ii) Replacing R = Me with R = Ph causes an approximate doubling of σ_2 in three out of four instances (with **9** providing the exception). However, the 2PA activity of the 2,4-DNPh derivative **12** is only about half that of **10**. (iii) The previously reported Fe compounds **7** and **9** show only very small σ_2 values, while their Ru analogues **1** and **3** are much more efficient two-photon absorbers.[16] However, the data for the new chromophores show that the effect of the metal center becomes less significant as the ligand π-systems are extended. Hence, the Ru bbpe-based species **2** and **4** have σ_2 values about twice those of their Fe counterparts **8** and **10**. The Me_2bbpb^{2+} complexes in **5** and **11** have indistinguishable 2PA efficiencies, while that of **6** is substantially larger than that of **13**.

Our new complex chromophores clearly show much larger σ_2 values in comparison with their previously reported counterparts, but it is also of interest to draw some comparisons with data obtained for other species. Girardot et al. have used two-photon excited luminescence measurements to determine a σ_2 value of 90 GM (at 750 nm) for a derivative of $[Ru^{II}(phen)_3]^{2+}$ with six fluorenyl substituents (**14**; Figure 9).[12a] The relatively low efficiency in this case is probably attributable to limited π-conjugation within the ligands due to twisting about the interannular bonds. Nonetheless, a complex related to **14**, with $\sigma_2 = 40$ GM at 740 nm, has recently been studied in vitro as a singlet oxygen generator for potential applications in photodynamic cancer therapy.[12c] Some of us have also used the Z-scan approach to derive much larger σ_2 values of 2200 ± 300 and 1900 ± 300 GM (at 765 nm) for the complexes **15** and **16** (Figure 9), respectively,[12b] which are of magnitude similar to that reported here for **6** (Table 7). It is interesting to note that although **15** contains shorter conjugated systems, its 2PA activity is close to that measured for **6**. Comparison with the σ_2 value of 720 GM for **2** indicates that replacing an electron-accepting *N*-methylpyridinium group with a di-*n*-butylamino donor enhances the 2PA activity approximately 3-fold. It therefore appears that such tris-chelate complexes give larger 2PA effects when these are associated with directionally opposed MLCT and ILCT transitions (the latter involving strong amino donors as in **14**), as opposed to codirectional MLCT and ILCT processes (the latter involving weak pyridyl donors as in **2**). However, it is probably inappropriate to speculate further without more extensive studies involving variations in the Z-scan measurement wavelength. Despite the relatively impressive σ_2 values for these new and related complexes, other studies with Cu^{I}-, Cd^{II}-, or Zn^{II}-based systems have afforded considerably larger activities, exceeding even 10^4 GM.[52] A similarly huge σ_2 value has recently been reported for a dendrimeric nonanuclear Ru^{II} σ-acetylide complex,[53] and appropriately substituted Zn^{II} porphyrin complexes, with their extensive π-systems, are also among the most active 2PA chromophores known.[54]

Conclusions

We have synthesized several new bpy-based proligands and used these to extend the family of pyridinium-substituted tris-chelate complexes of Ru^{II} or Fe^{II}. As the conjugated systems extend, the presence of intense, low-energy ILCT bands becomes more apparent in the electronic absorption spectra. The

(51) The β_{EN} values (10^{-32} esu) for (*E*)-4′-(dimethylamino)-*N*-phenyl-4-stilbazolium hexafluorophosphate and its 2,4-dinitrophenyl counterpart are 322.0 and 307.9, respectively. For the corresponding (*E*,*E*)-1,3-butadienyl-containing compounds, the respective values are 602.8 and 532.5. Changing the electron donor to a julolidinyl group gives a similar pattern in the β_{EN} values (10^{-32} esu): 420.4 (R = Ph) and 398.0 (R = 2,4-DNPh) for (*E*)-*N*-R-4-[2-(2,3,6,7-tetrahydro-1*H*,5*H*-pyrido[3,2,1-*ij*]quinolin-9-yl)vinyl]pyridinium hexafluorophosphate and 680.3 (R = Ph) and 663.0 (R = 2,4-DNPh) for the corresponding (*E*,*E*)-1,3-butadienyl compounds. Note also that the β_{EN} values for these pseudo-1D organic species are about 1 order of magnitude larger than those derived for the 3D tris-chelate complexes (Table 6).

(52) (a) Das, S.; Nag, A.; Goswami, D.; Bharadwaj, P. K. *J. Am. Chem. Soc.* **2006**, *128*, 402–403. (b) Jana, A.; Jang, S. Y.; Shin, J.-Y.; Kumar De, A.; Goswami, D.; Kim, D.; Bharadwaj, P. K. *Chem. Eur. J.* **2008**, *14*, 10628–10638.

(53) Roberts, R. L.; Schwich, T.; Corkery, T. C.; Cifuentes, M. P.; Green, K. A.; Farmer, J. D.; Low, P. J.; Marder, T. B.; Samoc, M.; Humphrey, M. G. *Adv. Mater.* **2009**, *21*, 2318–2322.

(54) (a) Drobizhev, M.; Stepanenko, Y.; Rebane, A.; Wilson, C. J.; Screen, T. E. O.; Anderson, H. L. *J. Am. Chem. Soc.* **2006**, *128*, 12432–12433. (b) Kim, K. S.; Noh, S. B.; Katsuda, T.; Ito, S.; Osuka, A.; Kim, D.-H. *Chem. Commun.* **2007**, 2479–2481. (c) Collini, E.; Mazzucato, S.; Zerbetto, M.; Ferrante, C.; Bozio, R.; Pizzotti, M.; Tessore, F.; Ugo, R. *Chem. Phys. Lett.* **2008**, *454*, 70–74. (d) Odom, S. A.; et al. *J. Am. Chem. Soc.* **2009**, *131*, 7510–7511. (e) Webster, S.; Odom, S. A.; Padilha, L. A.; Przhonska, O. V.; Peceli, D.; Hu, H.-H.; Nootz, G.; Kachkovski, A. D.; Matichak, J.; Barlow, S.; Anderson, H. L.; Marder, S. R.; Hagan, D. J.; Van Stryland, E. W. *J. Phys. Chem. B* **2009**, *113*, 14854–14867.

MLCT bands show red shifts on extending the π-conjugation, increasing the electron acceptor strength of the pyridinium groups, and/or replacing Ru with Fe. Cyclic voltammetry reveals reversible $M^{III/II}$ waves, but generally irreversible ligand-based reductions. The β responses determined by via HRS measurements at 800 and 1064 nm are very large (up to 5600×10^{-30} esu), but are strongly enhanced by resonance. Stark spectroscopic studies on the MLCT bands lead to estimated β_0 values as high as ca. 600×10^{-30} esu in one instance, which represent lower limits because the contributions associated with the ILCT bands are not taken into account in most cases. For the two compounds where the ILCT contributions are also amenable to Stark analysis, potentially record β_0 values as high as ca. 10^{-27} esu are determined. These indirectly derived NLO responses generally increase on extending the π-conjugation and increasing the electron-accepting strength of the ligands, and are much larger than those determined previously for related complexes.[15] However, no clear superiority of either Ru or Fe is evident. The measured dipole moment changes can be as large as ca. 34 D and show the expected dependence on conjugation path length. *Z*-scan measurements at 750 nm reveal high σ_2 values of up to 2500 GM; these are slightly larger than or similar to those measured for related electron-donor-substituted complexes,[12b] but are as much as an order of magnitude higher than the activities we have determined previously for pyridinium derivatives.[16] The new chromophores reported are therefore relatively rare examples of species that combine unusually high quadratic and cubic NLO effects with potentially redox-switchable transition metal centers.

Acknowledgment. We thank the EPSRC for support (grants EP/D070732 and EP/E000738) and also the Fund for Scientific Research-Flanders (FWO-V, G.0312.08), the University of Leuven (GOA/2006/3), the NSF (grant CHE-0802907, 'Powering the Planet: an NSF Center for Chemical Innovation') and the Foundation for Polish Science. I.A. is a postdoctoral fellow of the FWO-V and M.S. is a Laureate of the FNP Welcome programme.

Supporting Information Available: Crystallographic information in CIF format; Figures S1−S3; complete ref 54d (PDF). This material is available free of charge via the Internet at http://pubs.acs.org.

JA910538S